Reduced mitochondrial resilience enables non-canonical induction of apoptosis after TNF receptor signaling in virus-infected hepatocytes

Sandra Lampl[1,§], Marianne K. Janas[1,§], Sainitin Donakonda[1,§], Marcus Brugger[1], Kerstin Lohr[1], Annika Schneider[1], Katrin Manske[1], Laura E. Sperl[2,3], Jennifer Wettmarshausen[4,5], Constanze Müller[6], Melanie Laschinger[7], Daniel Hartmann[7], Norber Hüser[7], Fabiana Perrochi[4,5], Philippe Schmitt-Kopplin[6,8], Franz Hagn[2,3], Lars Zender[9], Veit Hornung[10], Christoph Borner[11], Andreas Pichlmair[12], Hamid Kashkar[13,14], Martin Klingenspor[14]5 Marco Prinz[16], Sabrina Schreiner[17], Marcus Conrad[18], Philipp J. Jost[19], Hans Zischka[20], Katja Steiger[21], Martin Krönke[13,14], Dietmar Zehn[22], Ulrike Protzer[12,17,23], Mathias Heikenwälder[24], Percy A. Knolle[1,22,§] & Dirk Wohlleber[1,§]

1. Institute of Molecular Immunology and Experimental Oncology, University Hospital München rechts der Isar; Technical University of Munich, Munich, Germany
2. Institute of Structural Biology, Helmholtz Zentrum Munich, Neuherberg, Germany
3. Structural Membrane Biochemistry, Bavarian NMR Center at the Department of Chemistry and Institute for Advanced Study, Technical University of Munich, Garching, Germany
4. Gene Center/Department of Biochemistry, Ludwig-Maximilians Universität München, Munich, Germany
5. Institute for Obesity and Diabetes, Helmholtz Zentrum München, Neuherberg, Germany
6. Research Unit Analytical Biogeochemistry, Helmholtz Zentrum München, Neuherberg, Germany
7. Clinic of Surgery, University Hospital München rechts der Isar; Technical University of Munich, Munich, Germany
8. Chair of Analytical Food Chemistry, Technical University of Munich, Freising-Weihenstephan, Germany
9. Division of Gastroenterology and Oncology, University Hospital Tübingen, Tübingen, Germany
10. Center for Integrated Protein Science (CIPSM), Gene Center and Department of Biochemistry, Ludwig-Maximilians-Universität München, München, Germany
11. Institute of Molecular Medicine and Cell Research, University of Freiburg, Freiburg, Germany
12. Institute of Virology, Technical University of Munich, Munich, Germany
13. Cologne Excellence Cluster on Cellular Stress Response in Aging-Associated Diseases, University of Cologne, Cologne, Germany
14. Institute for Microbiology and Hygiene, and Center of Molecular Medicine, University of Cologne, Cologne, Germany.
15. Molecular Nutritional Medicine, Else Kröner-Fresenius Center, Technical University of Munich, Freising-Weihenstephan, Germany
16. Institute of Neuropathology, Medical Faculty, University of Freiburg, Germany
17. Institute of Virology, Helmholtz-Zentrum München, Neuherberg, Germany
18. Institute of Developmental Genetics, Helmholtz Zentrum München, Neuherberg, Germany.
19. III. Medical Department for Hematology and Oncology, Klinikum rechts der Isar, Technical University of Munich, Munich, Germany
20. Institute of Molecular Toxicology and Pharmacology, Helmholtz Zentrum München/German Research Center for Environmental Health GmbH, Neuherberg, Germany.
21. Institute of Pathology, Technical University of Munich, Munich, Germany.
22. Institute of Physiology and Immunology, Technical University of Munich, Freising-Weihenstephan, Germany
23. German Center for Infection research (DZIF), Munich Partner Site, Germany
24. Institute of Chronic Inflammation and Cancer, German-Cancer-Research Center, Heidelberg, Germany

§ These authors contributed equally

Address for correspondence:
Prof. Percy A. Knolle, MD
Institute of Molecular Immunology and Experimental Oncology
University Hospital München rechts der Isar
Technical University of Munich, Ismaningerstr. 22
81675 Munich, Germany
e-mail: percy.knolle@tum.de

Tel: +49-89-4140-6920
Fax: +49-89-4140-6922

Keywords: TNF, hepatocyte apoptosis, mitochondrial function, mitochondrial permeability transition, anti-viral immunity

Electronic word count: 5963 words

Number of Figures and Tables: 7 Figures

Conflict of interest: We declare no conflict of interest.

Financial support:
This work was supported by grants from the DFG (project number 272983813 – TRR179 to PK and DW), EU FP7, MIP-DILI to PK. LS and FH are supported by the Helmholtz Zentrum München and the Helmholtz Society (VH-NG-1039). This work was supported by ERC grants to MH, VH and AP, and by DZIF Munich site support to PK, AP and UP

Authors' contribution:
SL, MKJ, SD, MB, KL, AS, KM, LES, JW, CM and DW performed the experiments, obtained and analyzed data; LZ, CB, VH, HK, MP, MC, PJ, ML, NH, DH provided key reagents for conduct of experiments; SL, MKJ, FP, PS, FH, HZ, SS, KS, UP, MH, MK, AP, PAK and DW analyzed data, drafted study design and wrote the manuscript. All authors reviewed the manuscript.

Abstract

Background & Aims: Selective elimination of virus-infected hepatocytes occurs through virus-specific CD8 T-cells recognizing peptide-loaded MHC molecules. Here, we report that virus-infected hepatocytes are also selectively eliminated through a cell-autonomous mechanism.

Methods: We generated recombinant adenoviruses and genetically modified mouse models to identify the molecular mechanisms determining TNF-induced hepatocyte apoptosis *in vivo* and used *in vivo* bioluminescence imaging, immunohistochemistry, immunoblot analysis, RNAseq/proteome /phosphoproteome analyses, bioinformatic analyses, mitochondrial function tests.

Results: We found that TNF precisely eliminated only virus-infected hepatocytes independent from local inflammation and activation of immune sensory receptors. TNF receptor I was equally relevant for NFkB activation in healthy and infected hepatocytes, but selectively mediated apoptosis in infected hepatocytes. Caspase 8 activation downstream of TNF receptor signaling was dispensable for apoptosis in virus-infected hepatocytes, indicating a so far unknown non-canonical cell-intrinsic pathway promoting apoptosis in hepatocytes. We identified a unique state of mitochondrial vulnerability in virus-infected hepatocytes as cause for this non-canonical induction of apoptosis through TNF. Mitochondria from virus-infected hepatocytes showed normal biophysical and bioenergetic functions, but were characterized by reduced resilience towards calcium challenge. In the presence of unchanged TNF induced signaling, ROS-mediated calcium release from the ER caused mitochondrial permeability transition and apoptosis, which identified a link between extrinsic death receptor signaling and cell-intrinsic mitochondrial-mediated caspase activation.

Conclusion: Our findings reveal a novel concept in immune surveillance by identifying a cell-autonomous cell defense mechanism to selectively eliminate virus-infected hepatocytes by mitochondrial permeability transition.

Lay summary: We identify a novel mechanism that mediates selective elimination of virus-infected hepatocytes that is facilitated by vulnerable mitochondria.

Introduction

The liver is known for its unique immune functions and ability to induce immune tolerance [1]. CD8 T cells can either receive tolerogenic signals to become non-responsive to further stimulation or execute their effector function in response to recognition of their specific antigen in the context of MHC class I molecules [2]. While the outcome of the former is induction of antigen-specific immune tolerance [3, 4], the execution of CD8 T cell effector functions supports control of viral infection in hepatocytes [2]. Such execution of effector function and killing of infected hepatocytes requires direct MHC class I-restricted activation by the target cells and further stimulatory signals to achieve full T cell activation [5]. However, also cross-presentation of hepatocyte-derived molecules through liver-resident antigen-presenting cell populations like liver sinusoidal endothelial cells also leads to killing of infected hepatocytes [6]. This indicated two fundamentally different effector mechanisms that mediate elimination of virus-infected hepatocytes and led us to characterize the molecular mechanisms that determine the elimination of virus-infected hepatocytes independent from direct contact with effector CD8 T cells.

After cognate antigen recognition on infected cells, effector CD8 T cells eliminate target cells through perforin mediated delivery of the pro-apoptotic molecule Granzyme B as well as FAS-L induced activation of death-receptor signaling [7]. Activated effector CD8 T cells also release death-inducing effector molecules, like tumor necrosis factor (TNF), which also mediates killing of infected hepatocytes [6]. However, signaling through the tumor necrosis factor (TNF) receptor (TNFR) is known to induce pro-survival NFκB-signaling through formation of membrane proximal signaling complexes [8-10]. Consequently, only after inhibition of NFκB-activation, cells became sensitive to TNF-induced death, indicating a dominant role of pro-survival over pro-apoptotic signals [11, 12]. Furthermore, signaling through the TNFR or through the death receptor FAS alone are not sufficient to induce death in hepatocytes, but release pro-apoptotic mitochondrial cytochrome C into the cytosol is required to initiate apoptosis [13]. For this, direct cleavage of caspase 8 downstream of the TNF receptor leads to cleavage and activation of caspase 8 to generate pro-apoptotic effector molecules. These can then cause mitochondrial damage to release cytochrome C and induction of hepatocyte death [14]. Thus, TNF induces both, pro-survival and pro-apoptotic signaling, the balance of which determine whether a cell undergoes apoptosis.

Here, we investigate how viral infection rendered hepatocytes sensitive to TNF-mediated death, and found a non-canonical pathway for induction of apoptosis that occurred in the presence of pro-survival NFkB activation and did not require caspase 8. We identify reduced mitochondrial resilience towards calcium as distinctive characteristic of virus-infected hepatocytes that was responsible for TNF-induced mitochondrial permeability transition to elicit apoptosis.

Material and Methods

Mice

Mice were purchased from Charles-River except as noted otherwise. All mice were maintained under specific-pathogen-free conditions according to guidelines of the Federation of Laboratory Animal Science Association. All experiments were approved by the "Regierung von Oberbayern". The following transgenic or knockout mouse lines were provided by the authors: OT-1 mice, TNFR1$^{flox/flox}$ mice, MLKL$^{-/-}$ and RIPK3$^{-/-}$, Casp8$^{flox/flox}$, ASC$^{-/-}$mice. Rag2$^{-/-}$xIL2Rγ$^{-/-}$ mice were provided by D.Saur (TUM) TRIF$^{-/-}$mice by A.Limmer (Bonn) and gp91$^{-/-}$mice by M.Krönke (Cologne). The TNFR1$^{flox/flox}$ mice were generated using CRISPR/Cas9 gene editing. Briefly, 80 ng/µl Cas9 protein, 10ng/ul sgRNA (GATCACAAGAGAGCCGGTCA and GACGTTAGGGGATAAGCAAT for TNFR1$^{flox/flox}$ mice; GCCAGGAAGTGGGTTACTTT and CCGTGTGCTTGGAACTCCAC for TNFR2$^{flox/flox}$ mice) and 5 ng/µl targeting vector DNA were injected into the pronucleus of C57BL/6J zygotes. Twenty-four hours later, two-cell stage embryos were transferred into the uteri of pseudo-pregnant female mice. Viable offspring were genotyped by PCR and sequencing. Male mice between 6-10 weeks of age were used for experiments.

Primary human hepatocytes

All experiments were approved by the ethics committee at TUM (564/18SAS and 232/19S). The study protocol conformed to the ethical guidelines of the World Medical Association (WMA) Declaration of Helsinki. Research using human liver tissue was performed in accordance with the regulations of the ethics committee and the ethical guidelines of the WMA Declaration of Helsinki. Informed written consent was obtained from each patient. Primary human hepatocytes (PHH) were isolated by liver perfusion, digestion, and mechanical dissection and filtration (100µm mesh), percoll density gradient centrifugation and viability was determined by trypan blue exclusion. PHH were seeded on plates coated with collagenR (Serva) in Williams E medium (insulin-transferrin-selenium, 1.5% bovine serum albumin, GlutaMAX™, penicillin/streptomycin (Gibco) and maintained at 5% CO2 and 37°C.

Results

TNF-induced apoptosis in virus-infected hepatocytes

Elimination of virus-infected hepatocytes is achieved through CD8 T cells recognizing their specific antigen as processed peptide on MHC-class-I molecules. Here, we provide evidence for an effector mechanism selectively eliminating virus-infected hepatocytes independently from CD8 T cells using a preclinical viral infection-model with a hepatotropic recombinant adenovirus (Ad) containing a CMV-promoter driven expression-cassette coding for green-fluorescent-protein and luciferase (Ad-CMV-GL) to detect infected hepatocytes (**suppl.Fig. 1A**). Strikingly, TNF-challenge caused liver damage in a dose-dependent fashion in adenovirus-infected, but not uninfected mice (**Fig. 1A,B, suppl.Fig. 1B**). TNF triggered liver damage also after infection with lymphocytic choriomeningitis virus (LCMV) (**Fig. 1C,D**). TNF-induced liver damage was not related to the transgenes expressed by recombinant adenoviruses (**suppl.Fig. 1C**).

TNF family members mediate death signals [15], but neither lymphotoxin, tumor-necrosis-factor-superfamily-member-14 (LIGHT), tumor-necrosis-factor-like-weak inducer-of-apoptosis (TWEAK) nor tumor-necrosis-factor-related-apoptosis-inducing-ligand (TRAIL) caused liver damage in infected mice (**Fig. 1E,F**). TNF elicited liver damage in Rag2xIL2-Receptor-$\gamma^{-/-}$ mice (deficient for T, B and NK-cells), in Fas-deficient(lpr) mice and after antibody-mediated granulocyte depletion (**suppl.Fig. 1D**), indicating that immune cells were not required. To confirm that hepatocyte-intrinsic mechanisms rather than increased effector cell function triggered death of virus-infected hepatocytes, we employed mice deficient for TNF receptors. Clearly, TNF receptor I knock-out ($TNFRI^{-/-}$) but not $TNFRII^{-/-}$ mice were protected (**Fig. 1G**), and human TNF, that exclusively signals through murine TNFRI [16], elicited liver damage (**Fig. 1H**). TNFRI-levels were similar before and after infection (**suppl.Fig. 1E**). To provide proof that TNFRI-signaling in virus-infected hepatocytes was required to trigger cell death, we generated transgenic $TNFRI^{flox/flox}$-mice using gene-editing. We then generated an adenovirus coding for Cre-recombinase in addition to GFP and luciferase (Ad-CMV-GCL) to selectively delete TNFRI in infected hepatocytes in $TNFRI^{flox/flox}$-mice. Strikingly, TNF application did not elicit liver damage in Ad-CMV-GCL-infected $TNFRI^{flox/flox}$-mice any more (**Fig. 1I**). Importantly, also in primary human hepatocytes infected with Ad-CMV-GL, TNF-challenge induced cell death shown by time-resolved measurements (**Fig. 1J**). In conclusion, TNFRI on virus-infected hepatocytes mediated cell death.

TNF induces different modes of cell death [17]. We neither found evidence for necroptosis, that requires the signaling molecules Receptor-Interacting serine/threonine-Protein Kinase 3 (Ripk3) or Mixed-Lineage-Kinase-Domain-Like-Pseudokinase (MLKL) [18], because TNF elicited liver damage in virus-infected $MLKL^{-/-}$ mice (**Fig. 1K**) and $Ripk3^{-/-}$ mice (**suppl.Fig. 1F**); nor for pyroptosis through inflammasome-activation requiring the Apoptosis-associated-Speck-like-protein containing-a-Caspase-

recruitment-domain (ASC) [19], because TNF induced liver damage in infected $ASC^{-/-}$ mice and after specific inhibition of caspase 1; nor for ferroptosis that is inhibited by liproxstatin, which did not prevent TNF-induced liver damage; nor for oxeiptosis requiring the mitochondrial-protein-phosphatase PGAM5, because TNF still induced liver damage in infected $PGAM5^{-/-}$ mice (**Fig. 1K**). However, blocking of initiator and effector caspases relevant for apoptosis induction through the pancaspase inhibitor Q-VD-OPh, reduced TNF-induced liver damage after infection (**Fig. 1L**). Consequently, we detected increased caspase-activation, high levels of cleaved caspases (casp) 8, 9 and 3, the truncated and pro-apoptotic form of the BH3-Interacting-Domain-death-agent (tBid) [20], and the cleaved form of the poly(ADP-ribose)-polymerase 1 (PARP) (**Fig. 1M, suppl.Fig. 1G**), a molecular marker of apoptosis [21]. Immunohistochemistry confirmed presence of cleaved-casp3 in infected hepatocytes (**Fig. 1L, suppl. Fig. 1H**). Thus, TNFRI-signaling induced apoptosis in virus-infected hepatocytes, and raised the question how such cell-autonomous sensitivity to TNF was achieved.

Canonical caspase-activation downstream of TNFR-signaling is dispensable for apoptosis in infected hepatocytes

Shifting the balance from NFκB-mediated pro-survival to pro-apoptotic signals during TNFR-signaling causes apoptosis [11]. However, in virus-infected as well as uninfected livers, TNF-challenge induced similar NFκB-activation, shown by decreased IκB-levels (**Fig. 2A**), nuclear translocation of the transcriptionally active form of NFκB (RelA) in infected GFP^{pos} and uninfected GFP^{neg} hepatocytes (**Fig. 2B**) and unchanged expression of the NFκB target gene *A20* (**suppl.Fig. 2A**), suggesting intact pro-survival signaling. Furthermore, anti-apoptotic molecules such as cellular-FLICE-like-inhibitor-protein (c-Flip), the cellular-Inhibitors-of-Apoptosis-Proteins (cIAPs) and the X-linked-inhibitor-of-apoptosis-protein (XIAP), that control casp8-cleavage and induction of apoptosis [12], were unchanged after infection (**suppl.Fig. 2B**). Importantly, although NFκB-signaling occurred within minutes after TNF-challenge in infected and noninfected hepatocytes, casp8-cleavage was found only after 45 minutes, together with casp3/9 and PARP-cleavage (**Fig. 2A,C**). Consistently, increased sALT levels were observed 2hrs after TNF-application (**Fig. 2D**). Rapid NFκB-activation and delayed caspase-cleavage suggested that apoptosis was independent from canonical pro-apoptotic TNFR-signaling, where reduced NFκB-activation leads to casp8-cleavage [14], and prompted us to investigate whether casp8-activation was necessary for TNF-induced death.

We selectively depleted casp8 from virus-infected hepatocytes by infecting $Casp8^{flox/flox}$ mice with Ad-CMV-GCL, that codes for Cre-recombinase, to delete the floxed Casp8-gene in infected hepatocytes. After Ad-CMV-GCL and Ad-CMV-GL infection of C57BL/6 mice, TNF induced liver damage equally well

(**suppl. Fig. 2C,D**), excluding a pro-apoptotic effect of Cre-recombinase. Strikingly, after Ad-CMV-GCL infection of Casp8$^{flox/flox}$ mice, TNF induced similar liver damage as Ad-CMV-GL infection (**Fig. 2E**) suggesting that casp8 was dispensable. We cannot formally exclude that TNF initiated necroptosis, but we detected cleaved casp3 in Ad-CMV-GCL-infected GFP^{pos}-hepatocytes in casp8$^{flox/flox}$ mice after TNF-challenge (**Fig. 2F**). Together, this demonstrated that casp8 was not required for TNF to induce Casp3-cleavage, and raised the question how extrinsic cell death through TNFRI-signaling occurred in the absence of casp8.

T*ranscriptional and post-transcriptional programing after virus-infection in hepatocytes*

Immune sensory receptors recognize viral infection and initiate anti-viral immunity, like expression of interferons (IFNs) or TNF [22]. However, TNF induced liver damage in virus-infected IFNα-receptor$^{-/-}$ and IFNγ-receptor$^{-/-}$ mice (**Fig. 3A**), thus excluding a role of IFNs. To investigate immune sensory receptors, we used mice deficient for the TIR-domain-containing-adaptor-protein-inducing-Interferon-beta (TRIF), Myeloid-differentiation-factor-88 (MyD88), that lack critical adapter molecules downstream of Toll-like-receptor signaling, Myeloid-differentiation-association-protein-5 (MDA) and Stimulator-of-Interferon-Genes (STING), that lack key cytosolic immune sensors. TNF induced liver damage after infection in all these knockout mice. (**Fig. 3A**). Thus, sensitization to TNF-induced apoptosis was not related to canonical innate immune sensing of infection, and led us to study (post)transcriptional responses.

Principal-component-analysis (PCA) revealed distinct clustering of differentially regulated genes after Ad-CMV-GL infection compared to uninfected liver (**suppl. Fig. 3B**). There were 356 significantly up- and 84 genes down-regulated (**suppl.Table I**). Using the Kyoto-Encyclopedia-of-Genes-and-Genomes (KEGG) pathway analysis, we identified five up-regulated and two downregulated pathways (**Fig. 3B, suppl.Table II**). Gene-set-enrichment-analysis (GSEA) identified a weak over-representation of Interferon-sensitive genes that was not detected by KEGG-analysis. There was a weak enrichment of apoptosis-related genes, among which cell-cycle and DNA-replication associated genes were most common, without evidence for ER-stress-related genes (**Fig. 3C, suppl.Table III**), confirmed by absence of ER-stress markers (**Fig. 3D**). The top 20 differentially regulated genes were mainly involved in DNA-replication or cell-cycle (**Fig. 3E**), like *Cdkn1A (p21)*, *Ccne1*, *Ube2c*, *Ccne2* or *Cdk1*. However, there was no evidence for hepatocyte proliferation, for cyclins or cell cycle completion (**suppl.Fig. 3C**). Transcription-factor-footprint-analysis confirmed enrichment of E2F2 and p53-related genes, and absence of NFκB-, mTOR- or CHOP-related genes (**Fig. 3F, suppl.Table III**). Of note, Foxo1-related genes were significantly down-regulated (**Fig. 3F**) implying metabolic changes after infection. Detection of p53-related genes by KEGG-pathway-analysis, GSEA and increased levels of phosphorylated-H2A-histone-family-member-X (γH2AX) (**Fig. 3E**) indicated a DNA-damage-responses known to occur after adenoviral infection [23]. We

therefore challenged infected $p21^{-/-}$ and $p53^{-/-}$-mice with TNF. Despite increased hepatic p53-phosphorylation and p21-levels after infection, TNF caused liver damage in both mouse-lines (**Fig. 3F**). These results did not reveal a pro-apoptotic transcriptional response after viral infection, and led us to study posttranscriptional events by performing proteome and phosphoproteome analyses.

A proteome analysis of infected liver tissue revealed 1187 differentially regulated proteins compared to uninfected liver (**Fig. 4A, suppl.Table IV**). Top 20 upregulated proteins and KEGG-analysis demonstrated over-representation of pathways associated with cell-cycle/replication (**Fig. 4B,C, supp.Table V**). Pathway-enrichment-analysis also detected apoptosis-related proteins such as casp7, casp8, Parp1/3 (**Figure 4B**), but for induction of apoptosis these proteins require proteolytic cleavage. To unravel protein-protein interactions determining cell function, we performed a protein interactome analysis employing the STRING database [24], which showed a large protein-protein interaction network and a scale-free network architecture (**suppl.Fig.4 A,B**). Further dissection by topology-analysis revealed five up-regulated proteins with the highest numbers of connections: the minichromosome-maintenance-protein-6 (Mcm6), the signal-peptidase-5 (Spc25), transforming-acidic-coiled-coil-containing-protein-3 (Tacc3), Replication-protein-A2 (Rpa2) and Thymidine-kinase-1 (Tk1) (**Fig. 4D**). Protein-protein-interaction-network-analysis for these proteins, grouped according to KEGG-pathway relation, showed enrichment for cell cycle/replication and metabolism but not apoptosis (**Fig. 4E**). However, we experimentally excluded a role of a changed cell-cycle in TNF-mediated apoptosis in infected hepatocytes. Therefore, metabolic processes rather appeared to be involved in the sensitization towards TNF-induced death

Phosphoproteomes from uninfected, infected and TNF-challenged livers showed differences by PCA (**Fig. 5A).** We detected 590 significantly different phospho-sites in infected liver, 507 after TNF challenge, and 431 following TNF challenge after infection (**suppl.Table VI**). Combining proteome and phosphoproteome results, a dynamic network analysis using the public SIGNOR database [25] predicted a prominent function of mTOR- and ErbB-signaling, which overlapped at two central signaling kinases (**Fig. 5B**, **suppl.Table VII**). Probing the phosphoproteome after TNF challenge, we found in infected but not uninfected liver phosphorylation of the kinase glycogen-synthase-kinase 3 (GSK3B) (**Fig. 5C,D**, **suppl.Table VII)**, which is involved in energy metabolism. To investigate signaling processes after TNF-challenge, we predicted motifs and kinases regulating the phosphoproteome using the iGPS-database [26]. This identified the same kinases in both, virus-infected and uninfected livers after TNF challenge (**Fig. 5E,F**, **suppl.Fig.5 A-J**), indicating that TNF-induced signaling was unchanged. Together, these data suggested that metabolic processes were involved in the sensitization towards TNF-induced death.

Conserved energy metabolism but decreased stress resilience in hepatocyte mitochondria after infection

We turned our attention to mitochondria, that are at the intersection of metabolism, cell signaling and death [27] and in hepatocytes are required for apoptosis induction [13]. The transcriptional changes in metabolic pathways e.g. pyrimidine metabolism and fatty acid metabolism, and upregulation of genes for Cyclin-dependent-kinase-1 (*Cdk1)*, Tubulin-beta-6 (*Tubb6)*, Rad51-recombinase (*Rad51)*, Thymidilate-synthase (*Tyms)*, Flap-structure-specific-endonuclease-1 (*Fen1)* and Methylen-tetrahydrofolate 2 (*Mthfd2)*, that are part of a mitochondrial stress signature [28, 29], suggested changes in mitochondrial integrity and function after infection. However, biophysical mitochondrial parameters, such as mitochondrial membrane fluidity or mitochondrial ultrastructure, were unchanged after infection (**Fig. 6A,B**). After infection, mitochondrial bioenergetic functions [30] were normal without changes in mitochondrial respiration or mitochondrial proton leak (**Fig. 6C** and **suppl.Fig. 6A-D**), indicating uncompromised mitochondrial bioenergetic functionality and biophysical integrity.

Hepatocyte apoptosis through death receptor-signaling requires mitochondrial release of cytochrome C [31]. After Ad-CMV-GL infection, we found increased levels of pro-apoptotic molecules, like Bcl2-like protein 11 (Bim) and Bcl2-like-protein-4 (Bax), whereas cytosolic levels of anti-apoptotic molecules like B-cell-lymphoma-extralarge (Bcl-XL) remained unchanged (**Fig. 6D**). This suggested a higher vulnerability of mitochondria from infected livers and prompted us to test mitochondrial stress resistance to tBid, that damages mitochondrial membranes to release cytochrome C [32]. Exposure to tBid caused mitochondria from infected livers to release more cytochrome C (**Fig. 6E, suppl.Fig. 6E**). Furthermore, oxygen consumption rates of ADP-exposed mitochondria slowed down over time (**Fig. 6F**), indicating decreased mitochondrial fitness. This suggested an increased vulnerability of mitochondria from infected cells to pro-apoptotic signals and led us to characterize how TNF receptor signaling linked mitochondria and apoptosis.

Vulnerable mitochondria undergoing rapid permeability transition upon ROS-signaling induced calcium challenge link TNF receptor signaling to induction of apoptosis in virus-infected hepatocytes

We next explored the role of TNF-induced activation of membrane proximal Nicotinamidadenin-dinukleotidephosphat (NADPH) oxidase (NOX1/2) that generates reactive-oxygen-species (ROS) [33]. ROS-scavenging by antioxidants like luteolin and trolox or ROS-degradation through adenoviral expression of superoxide dismutase reduced TNF-induced liver damage (**Fig. 7A,B**). ROS are also generated in mitochondria [34], but the mitochondria-targeting anti-oxidant mitoquinol mesylat (MitoQ) did not affect TNF-induced apoptosis (**Fig. 7C**). This pointed towards a critical role of membrane-proximal NADPH-oxidase in TNF-induced liver damage, which was confirmed by reduced TNF-induced liver damage in virus-infected $NOX2^{-/-}$-mice (**Fig. 7D**), then raising the question how TNF-induced ROS caused apoptosis. ROS activates phospholipase-Cγ to generate inositol-3-phosphate (IP_3) that triggers

calcium release from the ER through IP_3R-signaling [35]. Indeed, PLCγ-inhibition by edelfosine, blocking of IP_3-receptor signaling with xestospongine, and scavenging of intracellular calcium with BAPTA all reduced TNF-induced apoptosis (**Fig. 7E,F, suppl.Fig. 7**).

Mitochondrial calcium storage is key for cytosolic calcium homeostasis [36]. Strikingly, mitochondria from virus-infected livers displayed impaired calcium buffering capacity (**Fig. 7G**), pointing towards impaired mitochondrial calcium resilience. Importantly, after calcium challenge, mitochondria from infected livers showed rapid swelling and lost their membrane potential (**Fig. 7H**). Addition of cyclosporin-A (CsA), that inhibits mitochondrial cyclophilin D to trigger mitochondrial permeability transition (MPT) and cell death [37], prevented the calcium-induced mitochondrial swelling and loss of membrane potential (**Fig. 7H**). Thus, mitochondria of infected hepatocytes showed reduced resilience towards calcium challenges and suggested that ROS-induced calcium release triggered MPT. To determine whether MPT caused liver damage in infected mice after TNF challenge, we treated Ad-CMV-GL-infected mice with CsA, that prevents calcium-induced MPT [38]. Importantly, CsA reduced TNF-induced liver damage after infection (**Fig. 7I**). We reasoned that prevention of MPT also prevented caspase activation. Indeed, CsA reduced activation and casp3/casp8 cleavage in virus-infected livers (**Fig. 7J,K**), confirming the dispensable function of casp8 for TNF-induced apoptosis. Taken together, these results demonstrated that TNFRI-signaling in virus-infected hepatocytes elicited apoptosis through ROS-induced calcium release that mediated MPT and cytochrome C-release for caspase activation.

Discussion

Here we provide evidence for a cell-autonomous mechanism that mediates selective induction of apoptosis in virus-infected hepatocytes after TNFRI-signaling. This novel non-canonical pathway for induction of apoptosis linked extrinsic death receptor signaling by TNF through ROS production with intrinsic apoptosis induction through decreased mitochondrial resilience facilitating mitochondrial permeability transition. This achieved selective elimination of virus-infected hepatocytes.

Targeted elimination of infected hepatocytes is key to avoid immunopathology during antiviral CD8 T cell immunity [39], and induction and execution of virus-specific CD8 T cell effector functions are strongly controlled in the liver as tolerogenic organ [40]. Previously, virus-specific CD8 T cell killing of infected hepatocytes in the absence of direct MHC-restricted interaction was observed, that accounted for almost half of the total antiviral CD8 T cell activity [6], and raised the question how selective killing of infected cells through TNF was achieved. Our results provide evidence that neither canonical immune sensing of viral infection in cells through toll like receptors or cytosolic DNA-recognizing immune sensory receptors nor known cell stress conditions predisposed infected hepatocytes to TNF-induced apoptosis. Rather, we found that signaling downstream of TNFRI caused apoptosis in infected hepatocytes through

a non-canonical death pathway, which was independent from a shift from pro-survival to anti-apoptotic signaling and caspase 8 activation. Transcriptome and proteome profiling demonstrated subtle changes in metabolic processes after infection, but biophysical and bioenergetic functions of mitochondria remained uncompromised.

Mitochondria serve many functions ranging from energy supply through respiration, to metabolism, signaling and calcium homeostasis. The reduced stress resilience we found in mitochondria after viral infection was characterized by impaired calcium buffering capacity and increased vulnerability to undergo permeability transition upon calcium challenge. Sufficient calcium supply to mitochondria, however, is important to maintain high level respiration and ATP production through the electron transport chain [41, 42]. Close proximity of mitochondria and endoplasmatic reticulum (ER) as the main intracellular store of calcium, and their dedicated physical interaction sites together provide the necessary and dynamic calcium-supply for mitochondrial functions [41]. Viral gene expression may pose additional bioenergetic demands to infected hepatocytes, but we did not detect increased mitochondrial bioenergetic activity after infection. Multiple mechanisms regulate mitochondrial calcium uptake, storage and release [36, 43, 44], and this finely tuned process of mitochondrial calcium homeostasis may be modified upon virus infection in hepatocytes. Calcium is taken up by mitochondria through the calcium uniporter [45], and stored as calcium phosphate granules to buffer intra-mitochondrial calcium. However, kinetics and mechanisms of mitochondrial calcium storage and release remain largely unknown. Calcium-challenge in the context of reduced mitochondrial calcium-buffering capacity may cause calcium binding to cyclophilin D, which opens the permeability transition pore for cytochrome C release [36]. Thus, loss of calcium buffering capacity rather than accumulation of pro-apoptotic molecules or altered biophysical properties may explain increased mitochondrial vulnerability to calcium challenge observed in infected hepatocytes. The state of reduced mitochondrial resilience leaves their bioenergetic functionality intact and therefore allows infected hepatocytes to maintain their metabolic functions. However, reduced mitochondrial resilience towards calcium challenges as driving force for mitochondrial permeability transition allows selectively infected hepatocytes to respond to TNF receptor signaling with induction of apoptosis. The reduced mitochondrial resilience we identified adds a further level of protection for hepatocytes to detect viral infection also when viruses escape or overcome apoptotic signaling by the immune sensory pathways [46]. This mechanism may have evolved in hepatocytes to allow for selective elimination of virus-infected cells without causing collateral damage through immunopathology and to amplify the effector function of small numbers of antigen-specific CD8 T cells to eliminate a large number of infected cells in the liver.

In conclusion, our results define a novel concept of immune surveillance within infected cells, where reduced mitochondrial stress resilience serves as cell-autonomous mechanism that renders virus-infected cells sensitive to a non-canonical pathway of apoptosis induction.

Acknowledgments:

We thank Silke Hegenbarth (Institute of Molecular Immunology and Experimental Oncology, University Hospital München rechts der Isar), Sava Michailidou (Institute of Molecular Immunology and Experimental Oncology, University Hospital München rechts der Isar), Michaela Müller (Institute of Molecular Immunology and Experimental Oncology, University Hospital München rechts der Isar), Anne Jacob (Institute of Pathology, Technical University of Munich), Danijela Heide (Institute of Chronic Inflammation and Cancer, Deutsches Krebsforschungszentrum (DKFZ) Heidelberg), Theresa Asen (Institute of Virology, Technical University of Munich) and Antje Malo (Institute of Virology, Technical University of Munich) for their technical support. We thank Daniela Arduino (Gene Center/Department of Biochemistry, Ludwig-Maximilians Universität München) for protocols and technical support. We thank Sabine Schmitt and Carola Eberhagen (Institute of Molecular Toxicology and Pharmacology, Helmholtz Zentrum München) for performing electron microscopy.

References

Author names in bold designate shared co-first authorship.

[1] Knolle PA, Thimme R. Hepatic immune regulation and its involvement in viral hepatitis infection. Gastroenterology 2014;146:1193-1207.

[2] Thimme R, Wieland S, Steiger C, Ghrayeb J, Reimann KA, Purcell RH, et al. CD8(+) T cells mediate viral clearance and disease pathogenesis during acute hepatitis B virus infection. J Virol 2003;77:68-76.

[3] **Limmer A, Ohl J,** Kurts C, Ljunggren HG, Reiss Y, Groettrup M, et al. Efficient presentation of exogenous antigen by liver endothelial cells to CD8+ T cells results in antigen-specific T-cell tolerance. Nat Med 2000;6:1348-1354.

[4] Bertolino P, Bowen DG, McCaughan GW, Fazekas de St Groth B. Antigen-specific primary activation of CD8+ T cells within the liver. J Immunol 2001;166:5430-5438.

[5] Benechet AP, De Simone G, Di Lucia P, Cilenti F, Barbiera G, Le Bert N, et al. Dynamics and genomic landscape of CD8(+) T cells undergoing hepatic priming. Nature 2019;574:200-205.

[6] **Wohlleber D, Kashkar H, Gartner K,** Frings MK, Odenthal M, Hegenbarth S, et al. TNF-Induced Target Cell Killing by CTL Activated through Cross-Presentation. Cell reports 2012;2:478-487.

[7] Zhang N, Bevan MJ. CD8(+) T cells: foot soldiers of the immune system. Immunity 2011;35:161-168.

[8] Gerlach B, Cordier SM, Schmukle AC, Emmerich CH, Rieser E, Haas TL, et al. Linear ubiquitination prevents inflammation and regulates immune signalling. Nature 2011;471:591-596.

[9] Kalliolias GD, Ivashkiv LB. TNF biology, pathogenic mechanisms and emerging therapeutic strategies. Nat Rev Rheumatol 2016;12:49-62.

[10] **Peltzer N, Darding M,** Montinaro A, Draber P, Draberova H, Kupka S, et al. LUBAC is essential for embryogenesis by preventing cell death and enabling haematopoiesis. Nature 2018;557:112-117.

[11] Leist M, Gantner F, Bohlinger I, Germann PG, Tiegs G, Wendel A. Murine hepatocyte apoptosis induced in vitro and in vivo by TNF-alpha requires transcriptional arrest. J Immunol 1994;153:1778-1788.

[12] Varfolomeev E, Blankenship JW, Wayson SM, Fedorova AV, Kayagaki N, Garg P, et al. IAP antagonists induce autoubiquitination of c-IAPs, NF-kappaB activation, and TNFalpha-dependent apoptosis. Cell 2007;131:669-681.

[13] Jost PJ, Grabow S, Gray D, McKenzie MD, Nachbur U, Huang DC, et al. XIAP discriminates between type I and type II FAS-induced apoptosis. Nature 2009;460:1035-1039.

[14] Varfolomeev EE, Schuchmann M, Luria V, Chiannilkulchai N, Beckmann JS, Mett IL, et al. Targeted disruption of the mouse Caspase 8 gene ablates cell death induction by the TNF receptors, Fas/Apo1, and DR3 and is lethal prenatally. Immunity 1998;9:267-276.

[15] Walczak H. Death receptor-ligand systems in cancer, cell death, and inflammation. Cold Spring Harb Perspect Biol 2013;5:a008698.

[16] Lewis M, Tartaglia LA, Lee A, Bennett GL, Rice GC, Wong GH, et al. Cloning and expression of cDNAs for two distinct murine tumor necrosis factor receptors demonstrate one receptor is species specific. Proc Natl Acad Sci U S A 1991;88:2830-2834.

[17] Brenner D, Blaser H, Mak TW. Regulation of tumour necrosis factor signalling: live or let die. Nat Rev Immunol 2015;15:362-374.

[18] Cho YS, Challa S, Moquin D, Genga R, Ray TD, Guildford M, et al. Phosphorylation-driven assembly of the RIP1-RIP3 complex regulates programmed necrosis and virus-induced inflammation. Cell 2009;137:1112-1123.

[19] Man SM, Kanneganti TD. Converging roles of caspases in inflammasome activation, cell death and innate immunity. Nat Rev Immunol 2016;16:7-21.

[20] Li H, Zhu H, Xu CJ, Yuan J. Cleavage of BID by caspase 8 mediates the mitochondrial damage in the Fas pathway of apoptosis. Cell 1998;94:491-501.

[21] Simbulan-Rosenthal CM, Rosenthal DS, Iyer S, Boulares AH, Smulson ME. Transient poly(ADP-ribosyl)ation of nuclear proteins and role of poly(ADP-ribose) polymerase in the early stages of apoptosis. The Journal of biological chemistry 1998;273:13703-13712.

[22] Ivashkiv LB, Donlin LT. Regulation of type I interferon responses. Nat Rev Immunol 2014;14:36-49.

[23] Nichols GJ, Schaack J, Ornelles DA. Widespread phosphorylation of histone H2AX by species C adenovirus infection requires viral DNA replication. J Virol 2009;83:5987-5998.

[24] Szklarczyk D, Morris JH, Cook H, Kuhn M, Wyder S, Simonovic M, et al. The STRING database in 2017: quality-controlled protein-protein association networks, made broadly accessible. Nucleic acids research 2017;45:D362-D368.

[25] Licata L, Lo Surdo P, Iannuccelli M, Palma A, Micarelli E, Perfetto L, et al. SIGNOR 2.0, the SIGnaling Network Open Resource 2.0: 2019 update. Nucleic acids research 2020;48:D504-D510.

[26] Song C, Ye M, Liu Z, Cheng H, Jiang X, Han G, et al. Systematic analysis of protein phosphorylation networks from phosphoproteomic data. Molecular & cellular proteomics : MCP 2012;11:1070-1083.

[27] Galluzzi L, Kepp O, Kroemer G. Mitochondria: master regulators of danger signalling. Nat Rev Mol Cell Biol 2012;13:780-788.

[28] Quiros PM, Prado MA, Zamboni N, D'Amico D, Williams RW, Finley D, et al. Multi-omics analysis identifies ATF4 as a key regulator of the mitochondrial stress response in mammals. J Cell Biol 2017;216:2027-2045.

[29] Melber A, Haynes CM. UPR(mt) regulation and output: a stress response mediated by mitochondrial-nuclear communication. Cell Res 2018;28:281-295.

[30] Divakaruni AS, Brand MD. The regulation and physiology of mitochondrial proton leak. Physiology (Bethesda) 2011;26:192-205.

[31] **Yin XM, Wang K, Gross A, Zhao Y, Zinkel S,** Klocke B, et al. Bid-deficient mice are resistant to Fas-induced hepatocellular apoptosis. Nature 1999;400:886-891.

[32] **Luo X, Budihardjo I,** Zou H, Slaughter C, Wang X. Bid, a Bcl2 interacting protein, mediates cytochrome c release from mitochondria in response to activation of cell surface death receptors. Cell 1998;94:481-490.

[33] Yazdanpanah B, Wiegmann K, Tchikov V, Krut O, Pongratz C, Schramm M, et al. Riboflavin kinase couples TNF receptor 1 to NADPH oxidase. Nature 2009;460:1159-1163.

[34] Murphy MP. How mitochondria produce reactive oxygen species. Biochem J 2009;417:1-13.

[35] Domijan AM, Kovac S, Abramov AY. Lipid peroxidation is essential for phospholipase C activity and the inositol-trisphosphate-related Ca(2)(+) signal. J Cell Sci 2014;127:21-26.

[36] De Stefani D, Rizzuto R, Pozzan T. Enjoy the Trip: Calcium in Mitochondria Back and Forth. Annu Rev Biochem 2016;85:161-192.

[37] Baines CP, Kaiser RA, Purcell NH, Blair NS, Osinska H, Hambleton MA, et al. Loss of cyclophilin D reveals a critical role for mitochondrial permeability transition in cell death. Nature 2005;434:658-662.

[38] Halestrap AP, Connern CP, Griffiths EJ, Kerr PM. Cyclosporin A binding to mitochondrial cyclophilin inhibits the permeability transition pore and protects hearts from ischaemia/reperfusion injury. Mol Cell Biochem 1997;174:167-172.

[39] **Welz M, Eickhoff S,** Abdullah Z, Trebicka J, Gartlan KH, Spicer JA, et al. Perforin inhibition protects from lethal endothelial damage during fulminant viral hepatitis. Nat Commun 2018;9:4805.

[40] Protzer U, Maini MK, Knolle PA. Living in the liver: hepatic infections. Nat Rev Immunol 2012;12:201-213.

[41] Rizzuto R, De Stefani D, Raffaello A, Mammucari C. Mitochondria as sensors and regulators of calcium signalling. Nat Rev Mol Cell Biol 2012;13:566-578.

[42] Spinelli JB, Haigis MC. The multifaceted contributions of mitochondria to cellular metabolism. Nature cell biology 2018;20:745-754.

[43] Finkel T, Menazza S, Holmstrom KM, Parks RJ, Liu J, Sun J, et al. The ins and outs of mitochondrial calcium. Circulation research 2015;116:1810-1819.

[44] Giorgi C, Marchi S, Pinton P. The machineries, regulation and cellular functions of mitochondrial calcium. Nat Rev Mol Cell Biol 2018;19:713-730.

[45] **Baughman JM, Perocchi F,** Girgis HS, Plovanich M, Belcher-Timme CA, Sancak Y, et al. Integrative genomics identifies MCU as an essential component of the mitochondrial calcium uniporter. Nature 2011;476:341-345.

[46] You Y, Cheng AC, Wang MS, Jia RY, Sun KF, Yang Q, et al. The suppression of apoptosis by alpha-herpesvirus. Cell Death Dis 2017;8:e2749.

Figure legends

Figure 1 ***TNFR-signaling induces apoptosis selectively in virus-infected hepatocytes***

Experiments at d2 p.i. (Ad-CMV-GL) unless indicated differently and sALT levels at 4hrs after TNF-challenge. (**A-D**) sALT after i.v.-injection of murine TNF (400 ng/mouse) in Ad-CMV-GL (**A**) or LCMV-WE infected mice (**C**); H&E liver sections, arrows indicate dead hepatocytes, inset shows magnification of Ad-CMV-GL (**B**) or LCMV-WE infected mice (**D**), scale-bar: 100µm. (**E,F**) Challenge with TNFR-superfamily agonists. (**G**) TNF-challenge in infected $TNFRI^{-/-}$ or $TNFRII^{-/-}$ mice. (**H**) sALT after human TNF (400 ng/mouse). (**I**) Infection of $TNFRI^{flox/flox}$ mice with Ad-CMV-GCL. (**J**) TNF-challenge of primary human hepatocytes infected with Ad-CMV-GL and cell death-monitoring using impedance-measurement. (**K**) Infection and TNF-challenge of different knockout mice or mice pre-treated with different inhibitors for 30 minutes. (**L**) Blockade of apoptosis with pancaspase-inhibitor Q-VD-OPh. (**M**) Immunoblot of liver lysates for detection of full-length and cleaved caspases (casp), Bid and PARP-cleavage, or β-actin as loading control. (**N**) Liver immunohistochemistry for anti-GFP (red) and cleaved-casp3 (brown); inset shows magnification, scale-bar: 100µm. Results from representative experiments (n≥3), group size ≥4 mice, data are shown as mean+SEM. Unpaired t-test was used to calculate statistical significance, ns not significant, * p≤0.05, ** p≤0.01 and *** p≤0.001.

Figure 2 **TNF-challenge triggers apoptosis despite NFκB-signaling independent of casp8**

(**A-E**) Analysis at d2 p.i. (Ad-CMV-GL). (**A**) IκB-levels at 1hr after TNF by immunoblot from liver lysates. (**B**) Liver immunohistochemistry for nuclear RelA (brown) and infected GFP^{pos}-hepatocytes (red) at 1hr after TNF; scale bar 100µm. (**C**) Time kinetics of IκB-phosphorylation, casp and PARP-cleavage after TNF-treatment by immunoblot. (**D**) sALT time-kinetics after TNF-application in virus-infected mice. (**E**) sALT at 4hrs after TNF in Ad-CMV-GL or Ad-CMV-GCL-infected $Casp8^{flox/flox}$-mice; (**F**) Liver immunohistochemistry for cleaved casp3 (brown) and infected GFP^{pos}-hepatocytes (red) at 1hr after TNF in Ad-CMV-GL or Ad-CMV-GCL infected $Casp8^{flox/flox}$-mice; scale bar: 100µm. (**F**) Group size ≥4 mice, data shown as mean+SEM, unpaired t-test was used to calculate statistical significance. ns not significant. Results from representative experiments (n≥3).

Figure 3: **Transcriptional profiling of virus-infected liver does not reveal activation of pro-apoptotic pathways**

(**A**) sALT levels 4hrs after TNF-application in infected knockout mice. (**B,C**) Transcriptome analysis of whole liver mRNA from uninfected and Ad-CMV-GL-infected mice. (**B**) KEGG-pathway-analysis. (**C**) GSEA for ISGs, apoptosis- and ER stress-related genes. (**D**) ER-stress markers detected by immunoblot or PCR-

analysis from liver tissue (d2 p.i. with Ad-CMV-GL, tunicamycin treatment as positive control. (**E**) top 20 up-regulated genes from virus-infected liver. (**F**) Transcription-factor-footprint-analysis. (**G**) DNA-damage-response marker γ-H2AX by immunoblot from liver tissue at d2 p.i. (**H**) sALT at 4hrs after TNF in $p21^{-/-}$ or $p53^{-/-}$-mice. Results from representative experiments (n≥3), group size ≥4 mice, data are shown as mean+SEM. Unpaired t-test was used to calculate statistical significance. ns not significant.

Figure 4: **Over-representation of cell-cycle and DNA replication associated proteins after viral infection.**

(**A**) Heatmap of differentially expressed proteins in liver at d2 p.i. compared to uninfected liver. (**B**) Top 20 upregulated proteins in virus-infected livers. (**C**) KEGG-pathway-analysis for differentially expressed proteins after infection. (**D**) topology analysis of up-regulated protein-protein network in infected liver. (**E**) Visualization of the protein-protein interaction network in infected compared to uninfected liver built by STRING-database-analysis. Results from 4 independent experiments.

Figure 5: **Phosphoproteome analysis after virus infection**

(**A**) Principal component analysis of differential protein phosphorylation. (**B**) Dynamic network analysis of protein phosphorylation in virus-infected compared to uninfected liver grouped according to KEGG pathways. (**C,D**) Dynamic network analysis after TNF challenge. (**E**) Similarity analysis of the networks shown in (B-D) and quantified as Jaccard similarity coefficient. (**F**) Hierarchical analysis of upstream kinases involved in protein phosphorylation after TNF challenge. Results used for analysis were from 4 independent experiments.

Figure 6: ***Decreased mitochondrial stress resilience after viral infection***

(**A-F**) Analysis of mitochondria from livers at d2 p.i. (**A**) Ultrastructural analysis. (**B**) Mitochondrial membrane fluidity measured by fluorescence polarization of diphenylhexatriene (DPH). (**C**) Fold-change oxygen consumption rate (OCR) relative to basal OCR of isolated liver mitochondria using oxygen-flux-analysis, with succinate as substrate. (**D**) left: anti- and pro-apoptotic proteins by immunoblot of liver lysates; panel: immunoblot from liver mitochondria for Bax, mitochondrial marker cytochrome-C-oxidase-subunit-4 (COX IV) as loading control. (**E**) Cytochrome C by immunoblot from supernatants of liver mitochondria treated with tBid for 30 minutes or Triton X-100 for 10 minutes, COX IV and voltage-dependent-anion-channel (VDAC) as control for mitochondrial integrity. (**F**) OCR after ADP-addition as fold-change over time. Results from representative experiments (n≥3), data shown as mean+SEM. Unpaired t-test was used to calculate statistical significance, * p≤0.05 and ** p≤0.01.

Figure 7: **Mitochondrial permeability-transition links TNF challenge to apoptosis in virus-infected hepatocytes**

Analysis at d2 p.i. with Ad-CMV-GL and sALT levels 4hrs after TNF challenge (A-F). (**A**) Antioxidant treatment (30 minutes before TNF). (**B**) Ad-CMV-SOD infection (superoxide dismutase – neutralizing cytosolic ROS). (**C**) Neutralization of mitochondrial ROS using MitoQ (daily for six days, infection on d4 and analysis on d6). (**D**) gp91/NOX2$^{-/-}$-mice (**E**) inhibition of PLCγ-activity by edelfosine (0.5h before TNF). (**F**) treatment with calcium chelator BAPTA-AM (15 minutes before TNF). (**G**) Time kinetics of calcium-uptake by liver mitochondria after repetitive calcium challenges measured by Ca-Green-mediated detection of free calcium in supernatant. (**H**) Time kinetics of liver mitochondrial integrity (left) determined by changes in OD 540nm and mitochondrial membrane potential (right) determined by changes in Rh123-fluorescence intensity after calcium challenge. (**I**) sALT levels 4hrs after TNF challenge and inhibition of mitochondrial permeability transition with cyclosporin A (30 minutes before TNF). (**J,K**) Casp3 and casp8 activities in liver tissue at 1hr after TNF challenge (CsA 0.5h before TNF-treatment). Results from representative experiments (n≥3), group size ≥ 4 mice, data shown as mean+SEM, unpaired t-test was used to calculate statistical significance, ns not significant, * p≤0.05, ** p≤0.01 and *** p≤0.001.

Reduced mitochondrial resilience enables non-canonical induction of apoptosis after TNF receptor signaling in virus-infected hepatocytes

Sandra Lampl[1,§], Marianne K. Janas[1,§], Sainitin Donakonda[1,§], Marcus Brugger[1], Kerstin Lohr[1], Annika Schneider[1], Katrin Manske[1], Laura E. Sperl[2,3], Jennifer Wettmarshausen[4,5], Constanze Müller[6], Melanie Laschinger[7], Daniel Hartmann[7], Norber Hüser[7], Fabiana Perrochi[4,5], Philippe Schmitt-Kopplin[6,8], Franz Hagn[2,3], Lars Zender[9], Veit Hornung[10], Christoph Borner[11], Andreas Pichlmair[12], Hamid Kashkar[13,14], Martin Klingenspor[14]5 Marco Prinz[16], Sabrina Schreiner[17], Marcus Conrad[18], Philipp J. Jost[19], Hans Zischka[20], Katja Steiger[21], Martin Krönke[13,14], Dietmar Zehn[22], Ulrike Protzer[12,17,23], Mathias Heikenwälder[24], Percy A. Knolle[1,22,§] & Dirk Wohlleber[1,§]

1. Institute of Molecular Immunology and Experimental Oncology, University Hospital München rechts der Isar; Technical University of Munich, Munich, Germany
2. Institute of Structural Biology, Helmholtz Zentrum Munich, Neuherberg, Germany
3. Structural Membrane Biochemistry, Bavarian NMR Center at the Department of Chemistry and Institute for Advanced Study, Technical University of Munich, Garching, Germany
4. Gene Center/Department of Biochemistry, Ludwig-Maximilians Universität München, Munich, Germany
5. Institute for Obesity and Diabetes, Helmholtz Zentrum München, Neuherberg, Germany
6. Research Unit Analytical Biogeochemistry, Helmholtz Zentrum München, Neuherberg, Germany
7. Clinic of Surgery, University Hospital München rechts der Isar; Technical University of Munich, Munich, Germany
8. Chair of Analytical Food Chemistry, Technical University of Munich, Freising-Weihenstephan, Germany
9. Division of Gastroenterology and Oncology, University Hospital Tübingen, Tübingen, Germany
10. Center for Integrated Protein Science (CIPSM), Gene Center and Department of Biochemistry, Ludwig-Maximilians-Universität München, München, Germany
11. Institute of Molecular Medicine and Cell Research, University of Freiburg, Freiburg, Germany
12. Institute of Virology, Technical University of Munich, Munich, Germany
13. Cologne Excellence Cluster on Cellular Stress Response in Aging-Associated Diseases, University of Cologne, Cologne, Germany
14. Institute for Microbiology and Hygiene, and Center of Molecular Medicine, University of Cologne, Cologne, Germany.
15. Molecular Nutritional Medicine, Else Kröner-Fresenius Center, Technical University of Munich, Freising-Weihenstephan, Germany
16. Institute of Neuropathology, Medical Faculty, University of Freiburg, Germany
17. Institute of Virology, Helmholtz-Zentrum München, Neuherberg, Germany
18. Institute of Developmental Genetics, Helmholtz Zentrum München, Neuherberg, Germany.
19. III. Medical Department for Hematology and Oncology, Klinikum rechts der Isar, Technical University of Munich, Munich, Germany
20. Institute of Molecular Toxicology and Pharmacology, Helmholtz Zentrum München/German Research Center for Environmental Health GmbH, Neuherberg, Germany.
21. Institute of Pathology, Technical University of Munich, Munich, Germany.
22. Institute of Physiology and Immunology, Technical University of Munich, Freising-Weihenstephan, Germany
23. German Center for Infection research (DZIF), Munich Partner Site, Germany
24. Institute of Chronic Inflammation and Cancer, German-Cancer-Research Center, Heidelberg, Germany

§ These authors contributed equally

Address for correspondence:
Prof. Percy A. Knolle, MD
Institute of Molecular Immunology and Experimental Oncology
University Hospital München rechts der Isar
Technical University of Munich, Ismaningerstr. 22
81675 Munich, Germany
e-mail: percy.knolle@tum.de

Tel: +49-89-4140-6920
Fax: +49-89-4140-6922

Keywords: TNF, hepatocyte apoptosis, mitochondrial function, mitochondrial permeability transition, anti-viral immunity

Electronic word count: 5963 words

Number of Figures and Tables: 7 Figures

Conflict of interest: We declare no conflict of interest.

Financial support:
This work was supported by grants from the DFG (project number 272983813 – TRR179 to PK and DW), EU FP7, MIP-DILI to PK. LS and FH are supported by the Helmholtz Zentrum München and the Helmholtz Society (VH-NG-1039). This work was supported by ERC grants to MH, VH and AP, and by DZIF Munich site support to PK, AP and UP

Authors' contribution:
SL, MKJ, SD, MB, KL, AS, KM, LES, JW, CM and DW performed the experiments, obtained and analyzed data; LZ, CB, VH, HK, MP, MC, PJ, ML, NH, DH provided key reagents for conduct of experiments; SL, MKJ, FP, PS, FH, HZ, SS, KS, UP, MH, MK, AP, PAK and DW analyzed data, drafted study design and wrote the manuscript. All authors reviewed the manuscript.

Abstract

Background & Aims: Selective elimination of virus-infected hepatocytes occurs through virus-specific CD8 T-cells recognizing peptide-loaded MHC molecules. Here, we report that virus-infected hepatocytes are also selectively eliminated through a cell-autonomous mechanism.

Methods: We generated recombinant adenoviruses and genetically modified mouse models to identify the molecular mechanisms determining TNF-induced hepatocyte apoptosis *in vivo* and used *in vivo* bioluminescence imaging, immunohistochemistry, immunoblot analysis, RNAseq/proteome /phosphoproteome analyses, bioinformatic analyses, mitochondrial function tests.

Results: We found that TNF precisely eliminated only virus-infected hepatocytes independent from local inflammation and activation of immune sensory receptors. TNF receptor I was equally relevant for NFkB activation in healthy and infected hepatocytes, but selectively mediated apoptosis in infected hepatocytes. Caspase 8 activation downstream of TNF receptor signaling was dispensable for apoptosis in virus-infected hepatocytes, indicating a so far unknown non-canonical cell-intrinsic pathway promoting apoptosis in hepatocytes. We identified a unique state of mitochondrial vulnerability in virus-infected hepatocytes as cause for this non-canonical induction of apoptosis through TNF. Mitochondria from virus-infected hepatocytes showed normal biophysical and bioenergetic functions, but were characterized by reduced resilience towards calcium challenge. In the presence of unchanged TNF induced signaling, ROS-mediated calcium release from the ER caused mitochondrial permeability transition and apoptosis, which identified a link between extrinsic death receptor signaling and cell-intrinsic mitochondrial-mediated caspase activation.

Conclusion: Our findings reveal a novel concept in immune surveillance by identifying a cell-autonomous cell defense mechanism to selectively eliminate virus-infected hepatocytes by mitochondrial permeability transition.

Lay summary: We identify a novel mechanism that mediates selective elimination of virus-infected hepatocytes that is facilitated by vulnerable mitochondria.

Introduction

The liver is known for its unique immune functions and ability to induce immune tolerance [1]. CD8 T cells can either receive tolerogenic signals to become non-responsive to further stimulation or execute their effector function in response to recognition of their specific antigen in the context of MHC class I molecules [2]. While the outcome of the former is induction of antigen-specific immune tolerance [3, 4], the execution of CD8 T cell effector functions supports control of viral infection in hepatocytes [2]. Such execution of effector function and killing of infected hepatocytes requires direct MHC class I-restricted activation by the target cells and further stimulatory signals to achieve full T cell activation [5]. However, also cross-presentation of hepatocyte-derived molecules through liver-resident antigen-presenting cell populations like liver sinusoidal endothelial cells also leads to killing of infected hepatocytes [6]. This indicated two fundamentally different effector mechanisms that mediate elimination of virus-infected hepatocytes and led us to characterize the molecular mechanisms that determine the elimination of virus-infected hepatocytes independent from direct contact with effector CD8 T cells.

After cognate antigen recognition on infected cells, effector CD8 T cells eliminate target cells through perforin mediated delivery of the pro-apoptotic molecule Granzyme B as well as FAS-L induced activation of death-receptor signaling [7]. Activated effector CD8 T cells also release death-inducing effector molecules, like tumor necrosis factor (TNF), which also mediates killing of infected hepatocytes [6]. However, signaling through the tumor necrosis factor (TNF) receptor (TNFR) is known to induce pro-survival NFκB-signaling through formation of membrane proximal signaling complexes [8-10]. Consequently, only after inhibition of NFκB-activation, cells became sensitive to TNF-induced death, indicating a dominant role of pro-survival over pro-apoptotic signals [11, 12]. Furthermore, signaling through the TNFR or through the death receptor FAS alone are not sufficient to induce death in hepatocytes, but release pro-apoptotic mitochondrial cytochrome C into the cytosol is required to initiate apoptosis [13]. For this, direct cleavage of caspase 8 downstream of the TNF receptor leads to cleavage and activation of caspase 8 to generate pro-apoptotic effector molecules. These can then cause mitochondrial damage to release cytochrome C and induction of hepatocyte death [14]. Thus, TNF induces both, pro-survival and pro-apoptotic signaling, the balance of which determine whether a cell undergoes apoptosis.

Here, we investigate how viral infection rendered hepatocytes sensitive to TNF-mediated death, and found a non-canonical pathway for induction of apoptosis that occurred in the presence of pro-survival NFkB activation and did not require caspase 8. We identify reduced mitochondrial resilience towards calcium as distinctive characteristic of virus-infected hepatocytes that was responsible for TNF-induced mitochondrial permeability transition to elicit apoptosis.

Material and Methods

Mice

Mice were purchased from Charles-River except as noted otherwise. All mice were maintained under specific-pathogen-free conditions according to guidelines of the Federation of Laboratory Animal Science Association. All experiments were approved by the "Regierung von Oberbayern". The following transgenic or knockout mouse lines were provided by the authors: OT-1 mice, TNFR1$^{flox/flox}$ mice, MLKL$^{-/-}$ and RIPK3$^{-/-}$, Casp8$^{flox/flox}$, ASC$^{-/-}$mice. Rag2$^{-/-}$xIL2Rγ$^{-/-}$ mice were provided by D.Saur (TUM) TRIF$^{-/-}$mice by A.Limmer (Bonn) and gp91$^{-/-}$mice by M.Krönke (Cologne). The TNFR1$^{flox/flox}$ mice were generated using CRISPR/Cas9 gene editing. Briefly, 80 ng/µl Cas9 protein, 10ng/ul sgRNA (GATCACAAGAGAGCCGGTCA and GACGTTAGGGGATAAGCAAT for TNFR1$^{flox/flox}$ mice; GCCAGGAAGTGGGTTACTTT and CCGTGTGCTTGGAACTCCAC for TNFR2$^{flox/flox}$ mice) and 5 ng/µl targeting vector DNA were injected into the pronucleus of C57BL/6J zygotes. Twenty-four hours later, two-cell stage embryos were transferred into the uteri of pseudo-pregnant female mice. Viable offspring were genotyped by PCR and sequencing. Male mice between 6-10 weeks of age were used for experiments.

Primary human hepatocytes

All experiments were approved by the ethics committee at TUM (564/18SAS and 232/19S). The study protocol conformed to the ethical guidelines of the World Medical Association (WMA) Declaration of Helsinki. Research using human liver tissue was performed in accordance with the regulations of the ethics committee and the ethical guidelines of the WMA Declaration of Helsinki. Informed written consent was obtained from each patient. Primary human hepatocytes (PHH) were isolated by liver perfusion, digestion, and mechanical dissection and filtration (100µm mesh), percoll density gradient centrifugation and viability was determined by trypan blue exclusion. PHH were seeded on plates coated with collagenR (Serva) in Williams E medium (insulin-transferrin-selenium, 1.5% bovine serum albumin, GlutaMAX™, penicillin/streptomycin (Gibco) and maintained at 5% CO2 and 37°C.

Results

TNF-induced apoptosis in virus-infected hepatocytes

Elimination of virus-infected hepatocytes is achieved through CD8 T cells recognizing their specific antigen as processed peptide on MHC-class-I molecules. Here, we provide evidence for an effector mechanism selectively eliminating virus-infected hepatocytes independently from CD8 T cells using a preclinical viral infection-model with a hepatotropic recombinant adenovirus (Ad) containing a CMV-promoter driven expression-cassette coding for green-fluorescent-protein and luciferase (Ad-CMV-GL) to detect infected hepatocytes (**suppl.Fig. 1A**). Strikingly, TNF-challenge caused liver damage in a dose-dependent fashion in adenovirus-infected, but not uninfected mice (**Fig. 1A,B, suppl.Fig. 1B**). TNF triggered liver damage also after infection with lymphocytic choriomeningitis virus (LCMV) (**Fig. 1C,D**). TNF-induced liver damage was not related to the transgenes expressed by recombinant adenoviruses (**suppl.Fig. 1C**).

TNF family members mediate death signals [15], but neither lymphotoxin, tumor-necrosis-factor-superfamily-member-14 (LIGHT), tumor-necrosis-factor-like-weak inducer-of-apoptosis (TWEAK) nor tumor-necrosis-factor-related-apoptosis-inducing-ligand (TRAIL) caused liver damage in infected mice (**Fig. 1E,F**). TNF elicited liver damage in Rag2xIL2-Receptor-$\gamma^{-/-}$ mice (deficient for T, B and NK-cells), in Fas-deficient(lpr) mice and after antibody-mediated granulocyte depletion (**suppl.Fig. 1D**), indicating that immune cells were not required. To confirm that hepatocyte-intrinsic mechanisms rather than increased effector cell function triggered death of virus-infected hepatocytes, we employed mice deficient for TNF receptors. Clearly, TNF receptor I knock-out ($TNFRI^{-/-}$) but not $TNFRII^{-/-}$ mice were protected (**Fig. 1G**), and human TNF, that exclusively signals through murine TNFRI [16], elicited liver damage (**Fig. 1H**). TNFRI-levels were similar before and after infection (**suppl.Fig. 1E**). To provide proof that TNFRI-signaling in virus-infected hepatocytes was required to trigger cell death, we generated transgenic $TNFRI^{flox/flox}$-mice using gene-editing. We then generated an adenovirus coding for Cre-recombinase in addition to GFP and luciferase (Ad-CMV-GCL) to selectively delete TNFRI in infected hepatocytes in $TNFRI^{flox/flox}$-mice. Strikingly, TNF application did not elicit liver damage in Ad-CMV-GCL-infected $TNFRI^{flox/flox}$-mice any more (**Fig. 1I**). Importantly, also in primary human hepatocytes infected with Ad-CMV-GL, TNF-challenge induced cell death shown by time-resolved measurements (**Fig. 1J**). In conclusion, TNFRI on virus-infected hepatocytes mediated cell death.

TNF induces different modes of cell death [17]. We neither found evidence for necroptosis, that requires the signaling molecules Receptor-Interacting serine/threonine-Protein Kinase 3 (Ripk3) or Mixed-Lineage-Kinase-Domain-Like-Pseudokinase (MLKL) [18], because TNF elicited liver damage in virus-infected $MLKL^{-/-}$ mice (**Fig. 1K**) and $Ripk3^{-/-}$ mice (**suppl.Fig. 1F**); nor for pyroptosis through inflammasome-activation requiring the Apoptosis-associated-Speck-like-protein containing-a-Caspase-

recruitment-domain (ASC) [19], because TNF induced liver damage in infected $ASC^{-/-}$ mice and after specific inhibition of caspase 1; nor for ferroptosis that is inhibited by liproxstatin, which did not prevent TNF-induced liver damage; nor for oxeiptosis requiring the mitochondrial-protein-phosphatase PGAM5, because TNF still induced liver damage in infected $PGAM5^{-/-}$ mice (**Fig. 1K**). However, blocking of initiator and effector caspases relevant for apoptosis induction through the pancaspase inhibitor Q-VD-OPh, reduced TNF-induced liver damage after infection (**Fig. 1L**). Consequently, we detected increased caspase-activation, high levels of cleaved caspases (casp) 8, 9 and 3, the truncated and pro-apoptotic form of the BH3-Interacting-Domain-death-agent (tBid) [20], and the cleaved form of the poly(ADP-ribose)-polymerase 1 (PARP) (**Fig. 1M**, **suppl.Fig. 1G**), a molecular marker of apoptosis [21]. Immunohistochemistry confirmed presence of cleaved-casp3 in infected hepatocytes (**Fig. 1L, suppl. Fig. 1H**). Thus, TNFRI-signaling induced apoptosis in virus-infected hepatocytes, and raised the question how such cell-autonomous sensitivity to TNF was achieved.

Canonical caspase-activation downstream of TNFR-signaling is dispensable for apoptosis in infected hepatocytes

Shifting the balance from NFκB-mediated pro-survival to pro-apoptotic signals during TNFR-signaling causes apoptosis [11]. However, in virus-infected as well as uninfected livers, TNF-challenge induced similar NFκB-activation, shown by decreased IκB-levels (**Fig. 2A**), nuclear translocation of the transcriptionally active form of NFκB (RelA) in infected GFP^{pos} and uninfected GFP^{neg} hepatocytes (**Fig. 2B**) and unchanged expression of the NFκB target gene *A20* (**suppl.Fig. 2A**), suggesting intact pro-survival signaling. Furthermore, anti-apoptotic molecules such as cellular-FLICE-like-inhibitor-protein (c-Flip), the cellular-Inhibitors-of-Apoptosis-Proteins (cIAPs) and the X-linked-inhibitor-of-apoptosis-protein (XIAP), that control casp8-cleavage and induction of apoptosis [12], were unchanged after infection (**suppl.Fig. 2B**). Importantly, although NFκB-signaling occurred within minutes after TNF-challenge in infected and noninfected hepatocytes, casp8-cleavage was found only after 45 minutes, together with casp3/9 and PARP-cleavage (**Fig. 2A,C**). Consistently, increased sALT levels were observed 2hrs after TNF-application (**Fig. 2D**). Rapid NFκB-activation and delayed caspase-cleavage suggested that apoptosis was independent from canonical pro-apoptotic TNFR-signaling, where reduced NFκB-activation leads to casp8-cleavage [14], and prompted us to investigate whether casp8-activation was necessary for TNF-induced death.

We selectively depleted casp8 from virus-infected hepatocytes by infecting $Casp8^{flox/flox}$ mice with Ad-CMV-GCL, that codes for Cre-recombinase, to delete the floxed Casp8-gene in infected hepatocytes. After Ad-CMV-GCL and Ad-CMV-GL infection of C57BL/6 mice, TNF induced liver damage equally well

(**suppl. Fig. 2C,D**), excluding a pro-apoptotic effect of Cre-recombinase. Strikingly, after Ad-CMV-GCL infection of Casp8$^{flox/flox}$ mice, TNF induced similar liver damage as Ad-CMV-GL infection (**Fig. 2E**) suggesting that casp8 was dispensable. We cannot formally exclude that TNF initiated necroptosis, but we detected cleaved casp3 in Ad-CMV-GCL-infected GFP^{pos}-hepatocytes in casp8$^{flox/flox}$ mice after TNF-challenge (**Fig. 2F**). Together, this demonstrated that casp8 was not required for TNF to induce Casp3-cleavage, and raised the question how extrinsic cell death through TNFRI-signaling occurred in the absence of casp8.

T*ranscriptional and post-transcriptional programing after virus-infection in hepatocytes*

Immune sensory receptors recognize viral infection and initiate anti-viral immunity, like expression of interferons (IFNs) or TNF [22]. However, TNF induced liver damage in virus-infected IFNα-receptor$^{-/-}$ and IFNγ-receptor$^{-/-}$ mice (**Fig. 3A**), thus excluding a role of IFNs. To investigate immune sensory receptors, we used mice deficient for the TIR-domain-containing-adaptor-protein-inducing-Interferon-beta (TRIF), Myeloid-differentiation-factor-88 (MyD88), that lack critical adapter molecules downstream of Toll-like-receptor signaling, Myeloid-differentiation-association-protein-5 (MDA) and Stimulator-of-Interferon-Genes (STING), that lack key cytosolic immune sensors. TNF induced liver damage after infection in all these knockout mice. (**Fig. 3A**). Thus, sensitization to TNF-induced apoptosis was not related to canonical innate immune sensing of infection, and led us to study (post)transcriptional responses.

Principal-component-analysis (PCA) revealed distinct clustering of differentially regulated genes after Ad-CMV-GL infection compared to uninfected liver (**suppl. Fig. 3B**). There were 356 significantly up- and 84 genes down-regulated (**suppl.Table I**). Using the Kyoto-Encyclopedia-of-Genes-and-Genomes (KEGG) pathway analysis, we identified five up-regulated and two downregulated pathways (**Fig. 3B, suppl.Table II**). Gene-set-enrichment-analysis (GSEA) identified a weak over-representation of Interferon-sensitive genes that was not detected by KEGG-analysis. There was a weak enrichment of apoptosis-related genes, among which cell-cycle and DNA-replication associated genes were most common, without evidence for ER-stress-related genes (**Fig. 3C, suppl.Table III**), confirmed by absence of ER-stress markers (**Fig. 3D**). The top 20 differentially regulated genes were mainly involved in DNA-replication or cell-cycle (**Fig. 3E**), like *Cdkn1A (p21)*, *Ccne1*, *Ube2c*, *Ccne2* or *Cdk1*. However, there was no evidence for hepatocyte proliferation, for cyclins or cell cycle completion (**suppl.Fig. 3C**). Transcription-factor-footprint-analysis confirmed enrichment of E2F2 and p53-related genes, and absence of NFκB-, mTOR- or CHOP-related genes (**Fig. 3F, suppl.Table III**). Of note, Foxo1-related genes were significantly down-regulated (**Fig. 3F**) implying metabolic changes after infection. Detection of p53-related genes by KEGG-pathway-analysis, GSEA and increased levels of phosphorylated-H2A-histone-family-member-X (γH2AX) (**Fig. 3E**) indicated a DNA-damage-responses known to occur after adenoviral infection [23]. We

therefore challenged infected $p21^{-/-}$ and $p53^{-/-}$-mice with TNF. Despite increased hepatic p53-phosphorylation and p21-levels after infection, TNF caused liver damage in both mouse-lines (**Fig. 3F**). These results did not reveal a pro-apoptotic transcriptional response after viral infection, and led us to study posttranscriptional events by performing proteome and phosphoproteome analyses.

A proteome analysis of infected liver tissue revealed 1187 differentially regulated proteins compared to uninfected liver (**Fig. 4A, suppl.Table IV**). Top 20 upregulated proteins and KEGG-analysis demonstrated over-representation of pathways associated with cell-cycle/replication (**Fig. 4B,C, supp.Table V**). Pathway-enrichment-analysis also detected apoptosis-related proteins such as casp7, casp8, Parp1/3 (**Figure 4B**), but for induction of apoptosis these proteins require proteolytic cleavage. To unravel protein-protein interactions determining cell function, we performed a protein interactome analysis employing the STRING database [24], which showed a large protein-protein interaction network and a scale-free network architecture (**suppl.Fig.4 A,B**). Further dissection by topology-analysis revealed five up-regulated proteins with the highest numbers of connections: the minichromosome-maintenance-protein-6 (Mcm6), the signal-peptidase-5 (Spc25), transforming-acidic-coiled-coil-containing-protein-3 (Tacc3), Replication-protein-A2 (Rpa2) and Thymidine-kinase-1 (Tk1) (**Fig. 4D**). Protein-protein-interaction-network-analysis for these proteins, grouped according to KEGG-pathway relation, showed enrichment for cell cycle/replication and metabolism but not apoptosis (**Fig. 4E**). However, we experimentally excluded a role of a changed cell-cycle in TNF-mediated apoptosis in infected hepatocytes. Therefore, metabolic processes rather appeared to be involved in the sensitization towards TNF-induced death

Phosphoproteomes from uninfected, infected and TNF-challenged livers showed differences by PCA (**Fig. 5A).** We detected 590 significantly different phospho-sites in infected liver, 507 after TNF challenge, and 431 following TNF challenge after infection (**suppl.Table VI**). Combining proteome and phosphoproteome results, a dynamic network analysis using the public SIGNOR database [25] predicted a prominent function of mTOR- and ErbB-signaling, which overlapped at two central signaling kinases (**Fig. 5B**, **suppl.Table VII**). Probing the phosphoproteome after TNF challenge, we found in infected but not uninfected liver phosphorylation of the kinase glycogen-synthase-kinase 3 (GSK3B) (**Fig. 5C,D**, **suppl.Table VII)**, which is involved in energy metabolism. To investigate signaling processes after TNF-challenge, we predicted motifs and kinases regulating the phosphoproteome using the iGPS-database [26]. This identified the same kinases in both, virus-infected and uninfected livers after TNF challenge (**Fig. 5E,F**, **suppl.Fig.5 A-J**), indicating that TNF-induced signaling was unchanged. Together, these data suggested that metabolic processes were involved in the sensitization towards TNF-induced death.

Conserved energy metabolism but decreased stress resilience in hepatocyte mitochondria after infection

We turned our attention to mitochondria, that are at the intersection of metabolism, cell signaling and death [27] and in hepatocytes are required for apoptosis induction [13]. The transcriptional changes in metabolic pathways e.g. pyrimidine metabolism and fatty acid metabolism, and upregulation of genes for Cyclin-dependent-kinase-1 (*Cdk1)*, Tubulin-beta-6 (*Tubb6)*, Rad51-recombinase (*Rad51)*, Thymidilate-synthase (*Tyms)*, Flap-structure-specific-endonuclease-1 (*Fen1)* and Methylen-tetrahydrofolate 2 (*Mthfd2)*, that are part of a mitochondrial stress signature [28, 29], suggested changes in mitochondrial integrity and function after infection. However, biophysical mitochondrial parameters, such as mitochondrial membrane fluidity or mitochondrial ultrastructure, were unchanged after infection (**Fig. 6A,B**). After infection, mitochondrial bioenergetic functions [30] were normal without changes in mitochondrial respiration or mitochondrial proton leak (**Fig. 6C** and **suppl.Fig. 6A-D**), indicating uncompromised mitochondrial bioenergetic functionality and biophysical integrity.

Hepatocyte apoptosis through death receptor-signaling requires mitochondrial release of cytochrome C [31]. After Ad-CMV-GL infection, we found increased levels of pro-apoptotic molecules, like Bcl2-like protein 11 (Bim) and Bcl2-like-protein-4 (Bax), whereas cytosolic levels of anti-apoptotic molecules like B-cell-lymphoma-extralarge (Bcl-XL) remained unchanged (**Fig. 6D**). This suggested a higher vulnerability of mitochondria from infected livers and prompted us to test mitochondrial stress resistance to tBid, that damages mitochondrial membranes to release cytochrome C [32]. Exposure to tBid caused mitochondria from infected livers to release more cytochrome C (**Fig. 6E, suppl.Fig. 6E**). Furthermore, oxygen consumption rates of ADP-exposed mitochondria slowed down over time (**Fig. 6F**), indicating decreased mitochondrial fitness. This suggested an increased vulnerability of mitochondria from infected cells to pro-apoptotic signals and led us to characterize how TNF receptor signaling linked mitochondria and apoptosis.

Vulnerable mitochondria undergoing rapid permeability transition upon ROS-signaling induced calcium challenge link TNF receptor signaling to induction of apoptosis in virus-infected hepatocytes

We next explored the role of TNF-induced activation of membrane proximal Nicotinamidadenin-dinukleotidephosphat (NADPH) oxidase (NOX1/2) that generates reactive-oxygen-species (ROS) [33]. ROS-scavenging by antioxidants like luteolin and trolox or ROS-degradation through adenoviral expression of superoxide dismutase reduced TNF-induced liver damage (**Fig. 7A,B**). ROS are also generated in mitochondria [34], but the mitochondria-targeting anti-oxidant mitoquinol mesylat (MitoQ) did not affect TNF-induced apoptosis (**Fig. 7C**). This pointed towards a critical role of membrane-proximal NADPH-oxidase in TNF-induced liver damage, which was confirmed by reduced TNF-induced liver damage in virus-infected $NOX2^{-/-}$-mice (**Fig. 7D**), then raising the question how TNF-induced ROS caused apoptosis. ROS activates phospholipase-Cγ to generate inositol-3-phosphate (IP_3) that triggers

calcium release from the ER through IP_3R-signaling [35]. Indeed, PLCγ-inhibition by edelfosine, blocking of IP_3-receptor signaling with xestospongine, and scavenging of intracellular calcium with BAPTA all reduced TNF-induced apoptosis (**Fig. 7E,F, suppl.Fig. 7**).

Mitochondrial calcium storage is key for cytosolic calcium homeostasis [36]. Strikingly, mitochondria from virus-infected livers displayed impaired calcium buffering capacity (**Fig. 7G**), pointing towards impaired mitochondrial calcium resilience. Importantly, after calcium challenge, mitochondria from infected livers showed rapid swelling and lost their membrane potential (**Fig. 7H**). Addition of cyclosporin-A (CsA), that inhibits mitochondrial cyclophilin D to trigger mitochondrial permeability transition (MPT) and cell death [37], prevented the calcium-induced mitochondrial swelling and loss of membrane potential (**Fig. 7H**). Thus, mitochondria of infected hepatocytes showed reduced resilience towards calcium challenges and suggested that ROS-induced calcium release triggered MPT. To determine whether MPT caused liver damage in infected mice after TNF challenge, we treated Ad-CMV-GL-infected mice with CsA, that prevents calcium-induced MPT [38]. Importantly, CsA reduced TNF-induced liver damage after infection (**Fig. 7I**). We reasoned that prevention of MPT also prevented caspase activation. Indeed, CsA reduced activation and casp3/casp8 cleavage in virus-infected livers (**Fig. 7J,K**), confirming the dispensable function of casp8 for TNF-induced apoptosis. Taken together, these results demonstrated that TNFRI-signaling in virus-infected hepatocytes elicited apoptosis through ROS-induced calcium release that mediated MPT and cytochrome C-release for caspase activation.

Discussion

Here we provide evidence for a cell-autonomous mechanism that mediates selective induction of apoptosis in virus-infected hepatocytes after TNFRI-signaling. This novel non-canonical pathway for induction of apoptosis linked extrinsic death receptor signaling by TNF through ROS production with intrinsic apoptosis induction through decreased mitochondrial resilience facilitating mitochondrial permeability transition. This achieved selective elimination of virus-infected hepatocytes.

Targeted elimination of infected hepatocytes is key to avoid immunopathology during antiviral CD8 T cell immunity [39], and induction and execution of virus-specific CD8 T cell effector functions are strongly controlled in the liver as tolerogenic organ [40]. Previously, virus-specific CD8 T cell killing of infected hepatocytes in the absence of direct MHC-restricted interaction was observed, that accounted for almost half of the total antiviral CD8 T cell activity [6], and raised the question how selective killing of infected cells through TNF was achieved. Our results provide evidence that neither canonical immune sensing of viral infection in cells through toll like receptors or cytosolic DNA-recognizing immune sensory receptors nor known cell stress conditions predisposed infected hepatocytes to TNF-induced apoptosis. Rather, we found that signaling downstream of TNFRI caused apoptosis in infected hepatocytes through

a non-canonical death pathway, which was independent from a shift from pro-survival to anti-apoptotic signaling and caspase 8 activation. Transcriptome and proteome profiling demonstrated subtle changes in metabolic processes after infection, but biophysical and bioenergetic functions of mitochondria remained uncompromised.

Mitochondria serve many functions ranging from energy supply through respiration, to metabolism, signaling and calcium homeostasis. The reduced stress resilience we found in mitochondria after viral infection was characterized by impaired calcium buffering capacity and increased vulnerability to undergo permeability transition upon calcium challenge. Sufficient calcium supply to mitochondria, however, is important to maintain high level respiration and ATP production through the electron transport chain [41, 42]. Close proximity of mitochondria and endoplasmatic reticulum (ER) as the main intracellular store of calcium, and their dedicated physical interaction sites together provide the necessary and dynamic calcium-supply for mitochondrial functions [41]. Viral gene expression may pose additional bioenergetic demands to infected hepatocytes, but we did not detect increased mitochondrial bioenergetic activity after infection. Multiple mechanisms regulate mitochondrial calcium uptake, storage and release [36, 43, 44], and this finely tuned process of mitochondrial calcium homeostasis may be modified upon virus infection in hepatocytes. Calcium is taken up by mitochondria through the calcium uniporter [45], and stored as calcium phosphate granules to buffer intra-mitochondrial calcium. However, kinetics and mechanisms of mitochondrial calcium storage and release remain largely unknown. Calcium-challenge in the context of reduced mitochondrial calcium-buffering capacity may cause calcium binding to cyclophilin D, which opens the permeability transition pore for cytochrome C release [36]. Thus, loss of calcium buffering capacity rather than accumulation of pro-apoptotic molecules or altered biophysical properties may explain increased mitochondrial vulnerability to calcium challenge observed in infected hepatocytes. The state of reduced mitochondrial resilience leaves their bioenergetic functionality intact and therefore allows infected hepatocytes to maintain their metabolic functions. However, reduced mitochondrial resilience towards calcium challenges as driving force for mitochondrial permeability transition allows selectively infected hepatocytes to respond to TNF receptor signaling with induction of apoptosis. The reduced mitochondrial resilience we identified adds a further level of protection for hepatocytes to detect viral infection also when viruses escape or overcome apoptotic signaling by the immune sensory pathways [46]. This mechanism may have evolved in hepatocytes to allow for selective elimination of virus-infected cells without causing collateral damage through immunopathology and to amplify the effector function of small numbers of antigen-specific CD8 T cells to eliminate a large number of infected cells in the liver.

In conclusion, our results define a novel concept of immune surveillance within infected cells, where reduced mitochondrial stress resilience serves as cell-autonomous mechanism that renders virus-infected cells sensitive to a non-canonical pathway of apoptosis induction.

Acknowledgments:

We thank Silke Hegenbarth (Institute of Molecular Immunology and Experimental Oncology, University Hospital München rechts der Isar), Sava Michailidou (Institute of Molecular Immunology and Experimental Oncology, University Hospital München rechts der Isar), Michaela Müller (Institute of Molecular Immunology and Experimental Oncology, University Hospital München rechts der Isar), Anne Jacob (Institute of Pathology, Technical University of Munich), Danijela Heide (Institute of Chronic Inflammation and Cancer, Deutsches Krebsforschungszentrum (DKFZ) Heidelberg), Theresa Asen (Institute of Virology, Technical University of Munich) and Antje Malo (Institute of Virology, Technical University of Munich) for their technical support. We thank Daniela Arduino (Gene Center/Department of Biochemistry, Ludwig-Maximilians Universität München) for protocols and technical support. We thank Sabine Schmitt and Carola Eberhagen (Institute of Molecular Toxicology and Pharmacology, Helmholtz Zentrum München) for performing electron microscopy.

References

Author names in bold designate shared co-first authorship.

[1] Knolle PA, Thimme R. Hepatic immune regulation and its involvement in viral hepatitis infection. Gastroenterology 2014;146:1193-1207.

[2] Thimme R, Wieland S, Steiger C, Ghrayeb J, Reimann KA, Purcell RH, et al. CD8(+) T cells mediate viral clearance and disease pathogenesis during acute hepatitis B virus infection. J Virol 2003;77:68-76.

[3] **Limmer A, Ohl J,** Kurts C, Ljunggren HG, Reiss Y, Groettrup M, et al. Efficient presentation of exogenous antigen by liver endothelial cells to CD8+ T cells results in antigen-specific T-cell tolerance. Nat Med 2000;6:1348-1354.

[4] Bertolino P, Bowen DG, McCaughan GW, Fazekas de St Groth B. Antigen-specific primary activation of CD8+ T cells within the liver. J Immunol 2001;166:5430-5438.

[5] Benechet AP, De Simone G, Di Lucia P, Cilenti F, Barbiera G, Le Bert N, et al. Dynamics and genomic landscape of CD8(+) T cells undergoing hepatic priming. Nature 2019;574:200-205.

[6] **Wohlleber D, Kashkar H, Gartner K,** Frings MK, Odenthal M, Hegenbarth S, et al. TNF-Induced Target Cell Killing by CTL Activated through Cross-Presentation. Cell reports 2012;2:478-487.

[7] Zhang N, Bevan MJ. CD8(+) T cells: foot soldiers of the immune system. Immunity 2011;35:161-168.

[8] Gerlach B, Cordier SM, Schmukle AC, Emmerich CH, Rieser E, Haas TL, et al. Linear ubiquitination prevents inflammation and regulates immune signalling. Nature 2011;471:591-596.

[9] Kalliolias GD, Ivashkiv LB. TNF biology, pathogenic mechanisms and emerging therapeutic strategies. Nat Rev Rheumatol 2016;12:49-62.

[10] **Peltzer N, Darding M,** Montinaro A, Draber P, Draberova H, Kupka S, et al. LUBAC is essential for embryogenesis by preventing cell death and enabling haematopoiesis. Nature 2018;557:112-117.

[11] Leist M, Gantner F, Bohlinger I, Germann PG, Tiegs G, Wendel A. Murine hepatocyte apoptosis induced in vitro and in vivo by TNF-alpha requires transcriptional arrest. J Immunol 1994;153:1778-1788.

[12] Varfolomeev E, Blankenship JW, Wayson SM, Fedorova AV, Kayagaki N, Garg P, et al. IAP antagonists induce autoubiquitination of c-IAPs, NF-kappaB activation, and TNFalpha-dependent apoptosis. Cell 2007;131:669-681.

[13] Jost PJ, Grabow S, Gray D, McKenzie MD, Nachbur U, Huang DC, et al. XIAP discriminates between type I and type II FAS-induced apoptosis. Nature 2009;460:1035-1039.

[14] Varfolomeev EE, Schuchmann M, Luria V, Chiannilkulchai N, Beckmann JS, Mett IL, et al. Targeted disruption of the mouse Caspase 8 gene ablates cell death induction by the TNF receptors, Fas/Apo1, and DR3 and is lethal prenatally. Immunity 1998;9:267-276.

[15] Walczak H. Death receptor-ligand systems in cancer, cell death, and inflammation. Cold Spring Harb Perspect Biol 2013;5:a008698.

[16] Lewis M, Tartaglia LA, Lee A, Bennett GL, Rice GC, Wong GH, et al. Cloning and expression of cDNAs for two distinct murine tumor necrosis factor receptors demonstrate one receptor is species specific. Proc Natl Acad Sci U S A 1991;88:2830-2834.

[17] Brenner D, Blaser H, Mak TW. Regulation of tumour necrosis factor signalling: live or let die. Nat Rev Immunol 2015;15:362-374.

[18] Cho YS, Challa S, Moquin D, Genga R, Ray TD, Guildford M, et al. Phosphorylation-driven assembly of the RIP1-RIP3 complex regulates programmed necrosis and virus-induced inflammation. Cell 2009;137:1112-1123.

[19] Man SM, Kanneganti TD. Converging roles of caspases in inflammasome activation, cell death and innate immunity. Nat Rev Immunol 2016;16:7-21.

[20] Li H, Zhu H, Xu CJ, Yuan J. Cleavage of BID by caspase 8 mediates the mitochondrial damage in the Fas pathway of apoptosis. Cell 1998;94:491-501.

[21] Simbulan-Rosenthal CM, Rosenthal DS, Iyer S, Boulares AH, Smulson ME. Transient poly(ADP-ribosyl)ation of nuclear proteins and role of poly(ADP-ribose) polymerase in the early stages of apoptosis. The Journal of biological chemistry 1998;273:13703-13712.

[22] Ivashkiv LB, Donlin LT. Regulation of type I interferon responses. Nat Rev Immunol 2014;14:36-49.

[23] Nichols GJ, Schaack J, Ornelles DA. Widespread phosphorylation of histone H2AX by species C adenovirus infection requires viral DNA replication. J Virol 2009;83:5987-5998.

[24] Szklarczyk D, Morris JH, Cook H, Kuhn M, Wyder S, Simonovic M, et al. The STRING database in 2017: quality-controlled protein-protein association networks, made broadly accessible. Nucleic acids research 2017;45:D362-D368.

[25] Licata L, Lo Surdo P, Iannuccelli M, Palma A, Micarelli E, Perfetto L, et al. SIGNOR 2.0, the SIGnaling Network Open Resource 2.0: 2019 update. Nucleic acids research 2020;48:D504-D510.

[26] Song C, Ye M, Liu Z, Cheng H, Jiang X, Han G, et al. Systematic analysis of protein phosphorylation networks from phosphoproteomic data. Molecular & cellular proteomics : MCP 2012;11:1070-1083.

[27] Galluzzi L, Kepp O, Kroemer G. Mitochondria: master regulators of danger signalling. Nat Rev Mol Cell Biol 2012;13:780-788.

[28] Quiros PM, Prado MA, Zamboni N, D'Amico D, Williams RW, Finley D, et al. Multi-omics analysis identifies ATF4 as a key regulator of the mitochondrial stress response in mammals. J Cell Biol 2017;216:2027-2045.

[29] Melber A, Haynes CM. UPR(mt) regulation and output: a stress response mediated by mitochondrial-nuclear communication. Cell Res 2018;28:281-295.

[30] Divakaruni AS, Brand MD. The regulation and physiology of mitochondrial proton leak. Physiology (Bethesda) 2011;26:192-205.

[31] **Yin XM, Wang K, Gross A, Zhao Y, Zinkel S,** Klocke B, et al. Bid-deficient mice are resistant to Fas-induced hepatocellular apoptosis. Nature 1999;400:886-891.

[32] **Luo X, Budihardjo I,** Zou H, Slaughter C, Wang X. Bid, a Bcl2 interacting protein, mediates cytochrome c release from mitochondria in response to activation of cell surface death receptors. Cell 1998;94:481-490.

[33] Yazdanpanah B, Wiegmann K, Tchikov V, Krut O, Pongratz C, Schramm M, et al. Riboflavin kinase couples TNF receptor 1 to NADPH oxidase. Nature 2009;460:1159-1163.

[34] Murphy MP. How mitochondria produce reactive oxygen species. Biochem J 2009;417:1-13.

[35] Domijan AM, Kovac S, Abramov AY. Lipid peroxidation is essential for phospholipase C activity and the inositol-trisphosphate-related Ca(2)(+) signal. J Cell Sci 2014;127:21-26.

[36] De Stefani D, Rizzuto R, Pozzan T. Enjoy the Trip: Calcium in Mitochondria Back and Forth. Annu Rev Biochem 2016;85:161-192.

[37] Baines CP, Kaiser RA, Purcell NH, Blair NS, Osinska H, Hambleton MA, et al. Loss of cyclophilin D reveals a critical role for mitochondrial permeability transition in cell death. Nature 2005;434:658-662.

[38] Halestrap AP, Connern CP, Griffiths EJ, Kerr PM. Cyclosporin A binding to mitochondrial cyclophilin inhibits the permeability transition pore and protects hearts from ischaemia/reperfusion injury. Mol Cell Biochem 1997;174:167-172.

[39] **Welz M, Eickhoff S,** Abdullah Z, Trebicka J, Gartlan KH, Spicer JA, et al. Perforin inhibition protects from lethal endothelial damage during fulminant viral hepatitis. Nat Commun 2018;9:4805.

[40] Protzer U, Maini MK, Knolle PA. Living in the liver: hepatic infections. Nat Rev Immunol 2012;12:201-213.

[41] Rizzuto R, De Stefani D, Raffaello A, Mammucari C. Mitochondria as sensors and regulators of calcium signalling. Nat Rev Mol Cell Biol 2012;13:566-578.

[42] Spinelli JB, Haigis MC. The multifaceted contributions of mitochondria to cellular metabolism. Nature cell biology 2018;20:745-754.

[43] Finkel T, Menazza S, Holmstrom KM, Parks RJ, Liu J, Sun J, et al. The ins and outs of mitochondrial calcium. Circulation research 2015;116:1810-1819.

[44] Giorgi C, Marchi S, Pinton P. The machineries, regulation and cellular functions of mitochondrial calcium. Nat Rev Mol Cell Biol 2018;19:713-730.

[45] **Baughman JM, Perocchi F,** Girgis HS, Plovanich M, Belcher-Timme CA, Sancak Y, et al. Integrative genomics identifies MCU as an essential component of the mitochondrial calcium uniporter. Nature 2011;476:341-345.

[46] You Y, Cheng AC, Wang MS, Jia RY, Sun KF, Yang Q, et al. The suppression of apoptosis by alpha-herpesvirus. Cell Death Dis 2017;8:e2749.

Figure legends

Figure 1 ***TNFR-signaling induces apoptosis selectively in virus-infected hepatocytes***

Experiments at d2 p.i. (Ad-CMV-GL) unless indicated differently and sALT levels at 4hrs after TNF-challenge. (**A-D**) sALT after i.v.-injection of murine TNF (400 ng/mouse) in Ad-CMV-GL (**A**) or LCMV-WE infected mice (**C**); H&E liver sections, arrows indicate dead hepatocytes, inset shows magnification of Ad-CMV-GL (**B**) or LCMV-WE infected mice (**D**), scale-bar: 100µm. (**E,F**) Challenge with TNFR-superfamily agonists. (**G**) TNF-challenge in infected $TNFRI^{-/-}$ or $TNFRII^{-/-}$ mice. (**H**) sALT after human TNF (400 ng/mouse). (**I**) Infection of $TNFRI^{flox/flox}$ mice with Ad-CMV-GCL. (**J**) TNF-challenge of primary human hepatocytes infected with Ad-CMV-GL and cell death-monitoring using impedance-measurement. (**K**) Infection and TNF-challenge of different knockout mice or mice pre-treated with different inhibitors for 30 minutes. (**L**) Blockade of apoptosis with pancaspase-inhibitor Q-VD-OPh. (**M**) Immunoblot of liver lysates for detection of full-length and cleaved caspases (casp), Bid and PARP-cleavage, or β-actin as loading control. (**N**) Liver immunohistochemistry for anti-GFP (red) and cleaved-casp3 (brown); inset shows magnification, scale-bar: 100µm. Results from representative experiments (n≥3), group size ≥4 mice, data are shown as mean+SEM. Unpaired t-test was used to calculate statistical significance, ns not significant, * p≤0.05, ** p≤0.01 and *** p≤0.001.

Figure 2 **TNF-challenge triggers apoptosis despite NFκB-signaling independent of casp8**

(A-E) Analysis at d2 p.i. (Ad-CMV-GL). (**A**) IκB-levels at 1hr after TNF by immunoblot from liver lysates. (**B**) Liver immunohistochemistry for nuclear RelA (brown) and infected GFP^{pos}-hepatocytes (red) at 1hr after TNF; scale bar 100µm. (**C**) Time kinetics of IκB-phosphorylation, casp and PARP-cleavage after TNF-treatment by immunoblot. (**D**) sALT time-kinetics after TNF-application in virus-infected mice. (**E**) sALT at 4hrs after TNF in Ad-CMV-GL or Ad-CMV-GCL-infected $Casp8^{flox/flox}$-mice; (**F**) Liver immunohistochemistry for cleaved casp3 (brown) and infected GFP^{pos}-hepatocytes (red) at 1hr after TNF in Ad-CMV-GL or Ad-CMV-GCL infected $Casp8^{flox/flox}$-mice; scale bar: 100µm. (**F**) Group size ≥4 mice, data shown as mean+SEM, unpaired t-test was used to calculate statistical significance. ns not significant. Results from representative experiments (n≥3).

Figure 3: **Transcriptional profiling of virus-infected liver does not reveal activation of pro-apoptotic pathways**

(**A**) sALT levels 4hrs after TNF-application in infected knockout mice. (**B,C**) Transcriptome analysis of whole liver mRNA from uninfected and Ad-CMV-GL-infected mice. (**B**) KEGG-pathway-analysis. (**C**) GSEA for ISGs, apoptosis- and ER stress-related genes. (**D**) ER-stress markers detected by immunoblot or PCR-

analysis from liver tissue (d2 p.i. with Ad-CMV-GL, tunicamycin treatment as positive control. (**E**) top 20 up-regulated genes from virus-infected liver. (**F**) Transcription-factor-footprint-analysis. (**G**) DNA-damage-response marker γ-H2AX by immunoblot from liver tissue at d2 p.i. (**H**) sALT at 4hrs after TNF in $p21^{-/-}$ or $p53^{-/-}$-mice. Results from representative experiments (n≥3), group size ≥4 mice, data are shown as mean+SEM. Unpaired t-test was used to calculate statistical significance. ns not significant.

Figure 4: **Over-representation of cell-cycle and DNA replication associated proteins after viral infection.**

(**A**) Heatmap of differentially expressed proteins in liver at d2 p.i. compared to uninfected liver. (**B**) Top 20 upregulated proteins in virus-infected livers. (**C**) KEGG-pathway-analysis for differentially expressed proteins after infection. (**D**) topology analysis of up-regulated protein-protein network in infected liver. (**E**) Visualization of the protein-protein interaction network in infected compared to uninfected liver built by STRING-database-analysis. Results from 4 independent experiments.

Figure 5: **Phosphoproteome analysis after virus infection**

(**A**) Principal component analysis of differential protein phosphorylation. (**B**) Dynamic network analysis of protein phosphorylation in virus-infected compared to uninfected liver grouped according to KEGG pathways. (**C,D**) Dynamic network analysis after TNF challenge. (**E**) Similarity analysis of the networks shown in (B-D) and quantified as Jaccard similarity coefficient. (**F**) Hierarchical analysis of upstream kinases involved in protein phosphorylation after TNF challenge. Results used for analysis were from 4 independent experiments.

Figure 6: ***Decreased mitochondrial stress resilience after viral infection***

(**A-F**) Analysis of mitochondria from livers at d2 p.i. (**A**) Ultrastructural analysis. (**B**) Mitochondrial membrane fluidity measured by fluorescence polarization of diphenylhexatriene (DPH). (**C**) Fold-change oxygen consumption rate (OCR) relative to basal OCR of isolated liver mitochondria using oxygen-flux-analysis, with succinate as substrate. (**D**) left: anti- and pro-apoptotic proteins by immunoblot of liver lysates; panel: immunoblot from liver mitochondria for Bax, mitochondrial marker cytochrome-C-oxidase-subunit-4 (COX IV) as loading control. (**E**) Cytochrome C by immunoblot from supernatants of liver mitochondria treated with tBid for 30 minutes or Triton X-100 for 10 minutes, COX IV and voltage-dependent-anion-channel (VDAC) as control for mitochondrial integrity. (**F**) OCR after ADP-addition as fold-change over time. Results from representative experiments (n≥3), data shown as mean+SEM. Unpaired t-test was used to calculate statistical significance, * p≤0.05 and ** p≤0.01.

Figure 7: **Mitochondrial permeability-transition links TNF challenge to apoptosis in virus-infected hepatocytes**

Analysis at d2 p.i. with Ad-CMV-GL and sALT levels 4hrs after TNF challenge (A-F). (**A**) Antioxidant treatment (30 minutes before TNF). (**B**) Ad-CMV-SOD infection (superoxide dismutase – neutralizing cytosolic ROS). (**C**) Neutralization of mitochondrial ROS using MitoQ (daily for six days, infection on d4 and analysis on d6). (**D**) gp91/NOX2$^{-/-}$-mice (**E**) inhibition of PLCγ-activity by edelfosine (0.5h before TNF). (**F**) treatment with calcium chelator BAPTA-AM (15 minutes before TNF). (**G**) Time kinetics of calcium-uptake by liver mitochondria after repetitive calcium challenges measured by Ca-Green-mediated detection of free calcium in supernatant. (**H**) Time kinetics of liver mitochondrial integrity (left) determined by changes in OD 540nm and mitochondrial membrane potential (right) determined by changes in Rh123-fluorescence intensity after calcium challenge. (**I**) sALT levels 4hrs after TNF challenge and inhibition of mitochondrial permeability transition with cyclosporin A (30 minutes before TNF). (**J,K**) Casp3 and casp8 activities in liver tissue at 1hr after TNF challenge (CsA 0.5h before TNF-treatment). Results from representative experiments (n≥3), group size ≥ 4 mice, data shown as mean+SEM, unpaired t-test was used to calculate statistical significance, ns not significant, * p≤0.05, ** p≤0.01 and *** p≤0.001.

Figure 1

Click here to access/download;Figure;Figure 1 .tiff

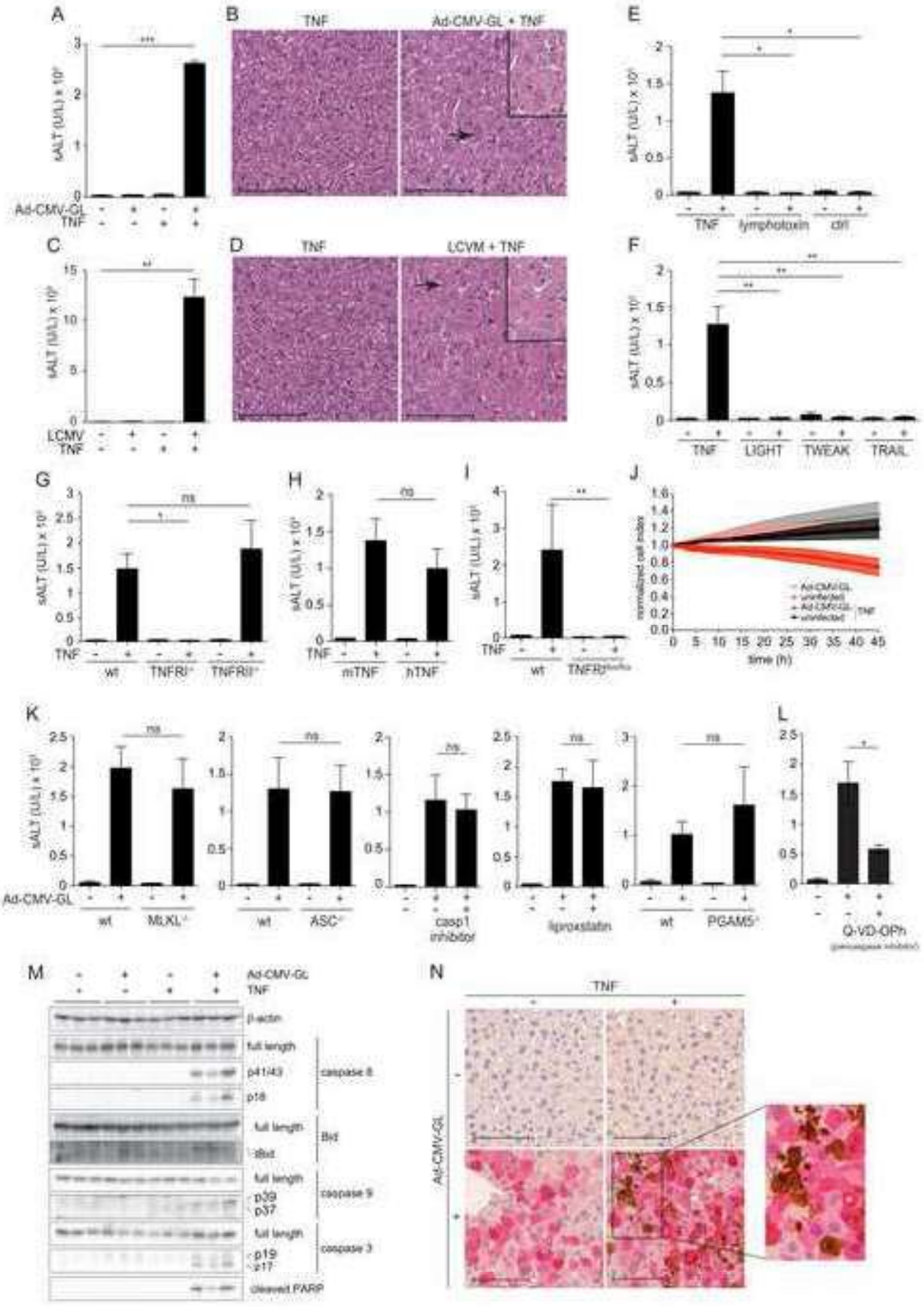

Figure 2

Click here to access/download;Figure;Figure 2 .tiff

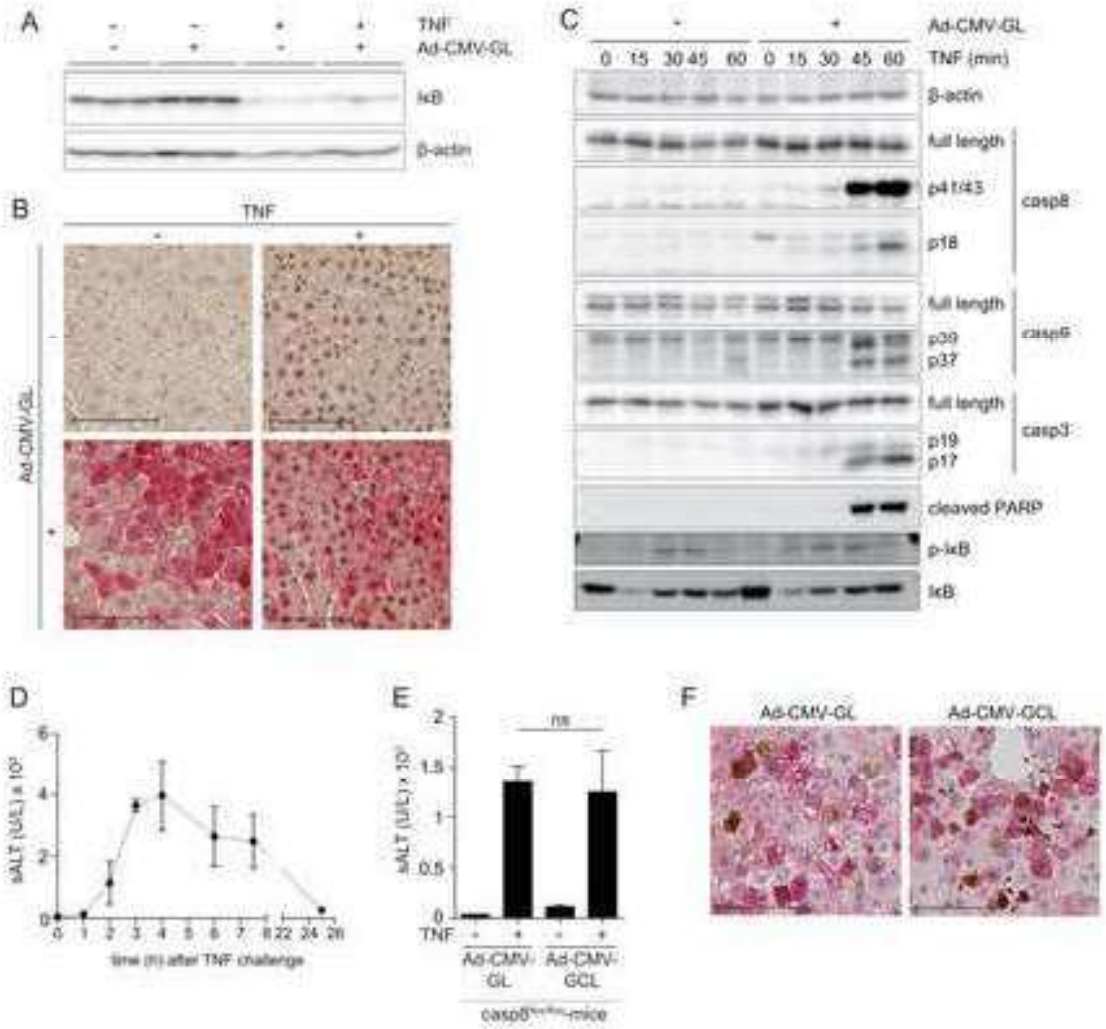

Figure 3

Click here to access/download;Figure;Figure 3 .tiff

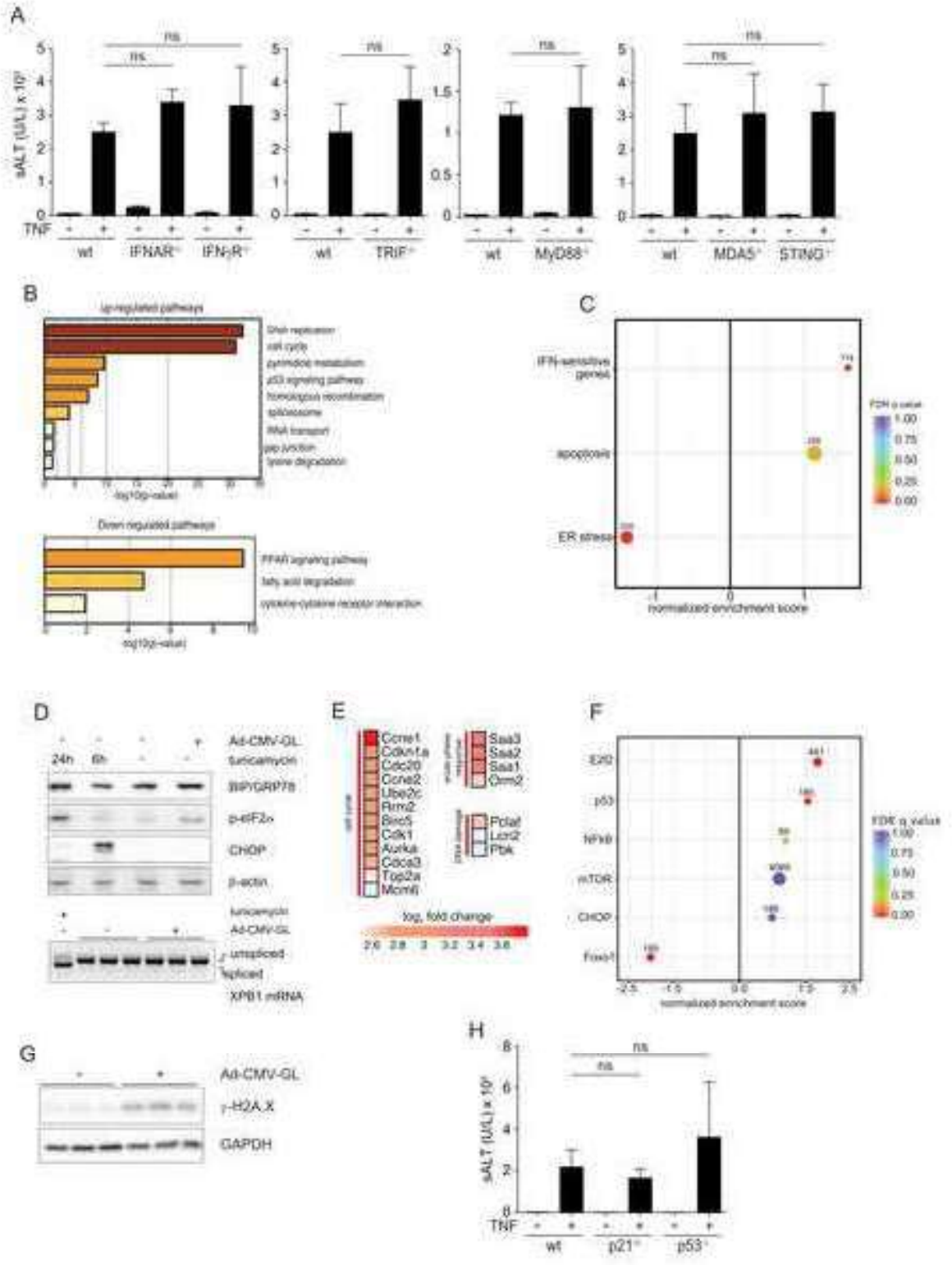

Figure 4

Click here to access/download;Figure;Figure 4 .tiff

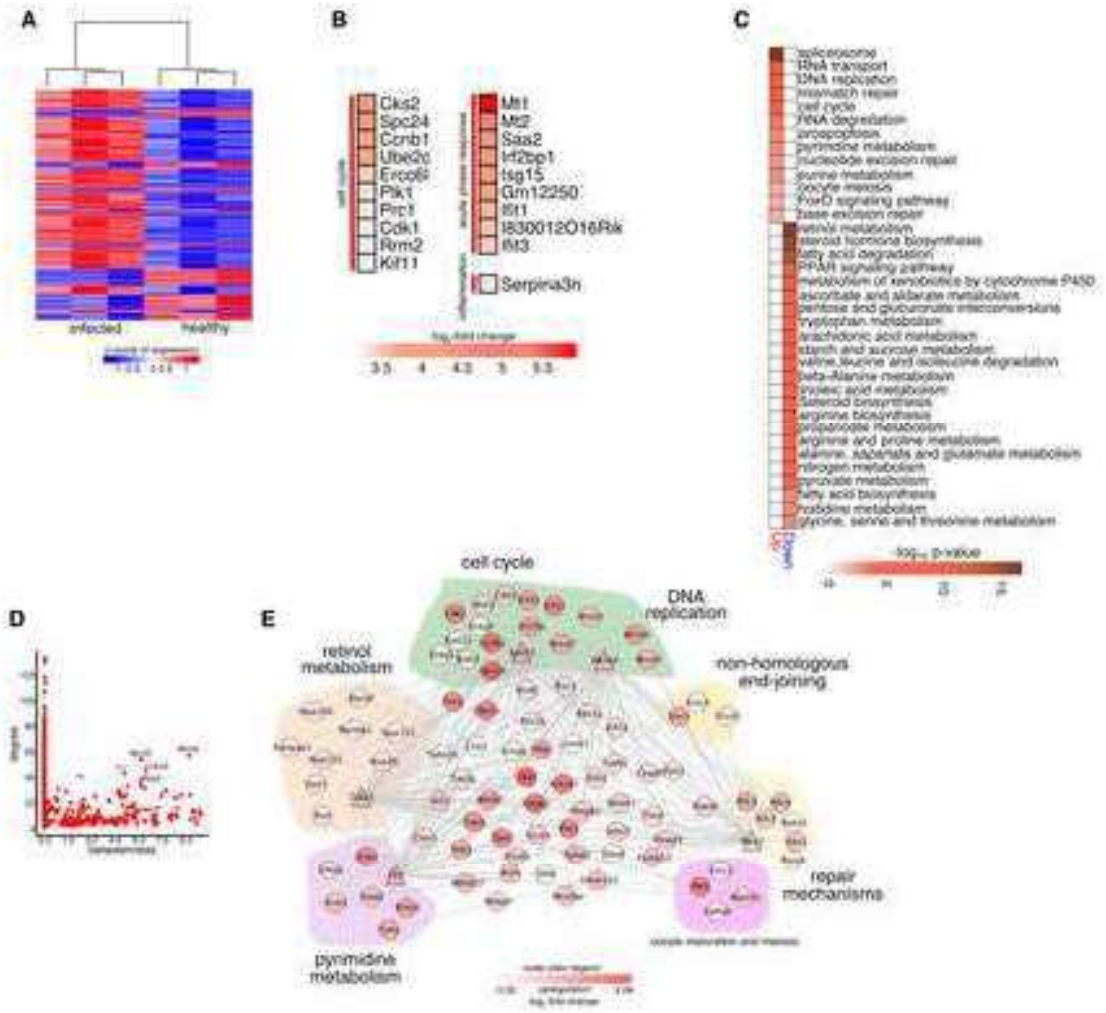

Figure 5

Click here to access/download;Figure;Figure 5 .tiff

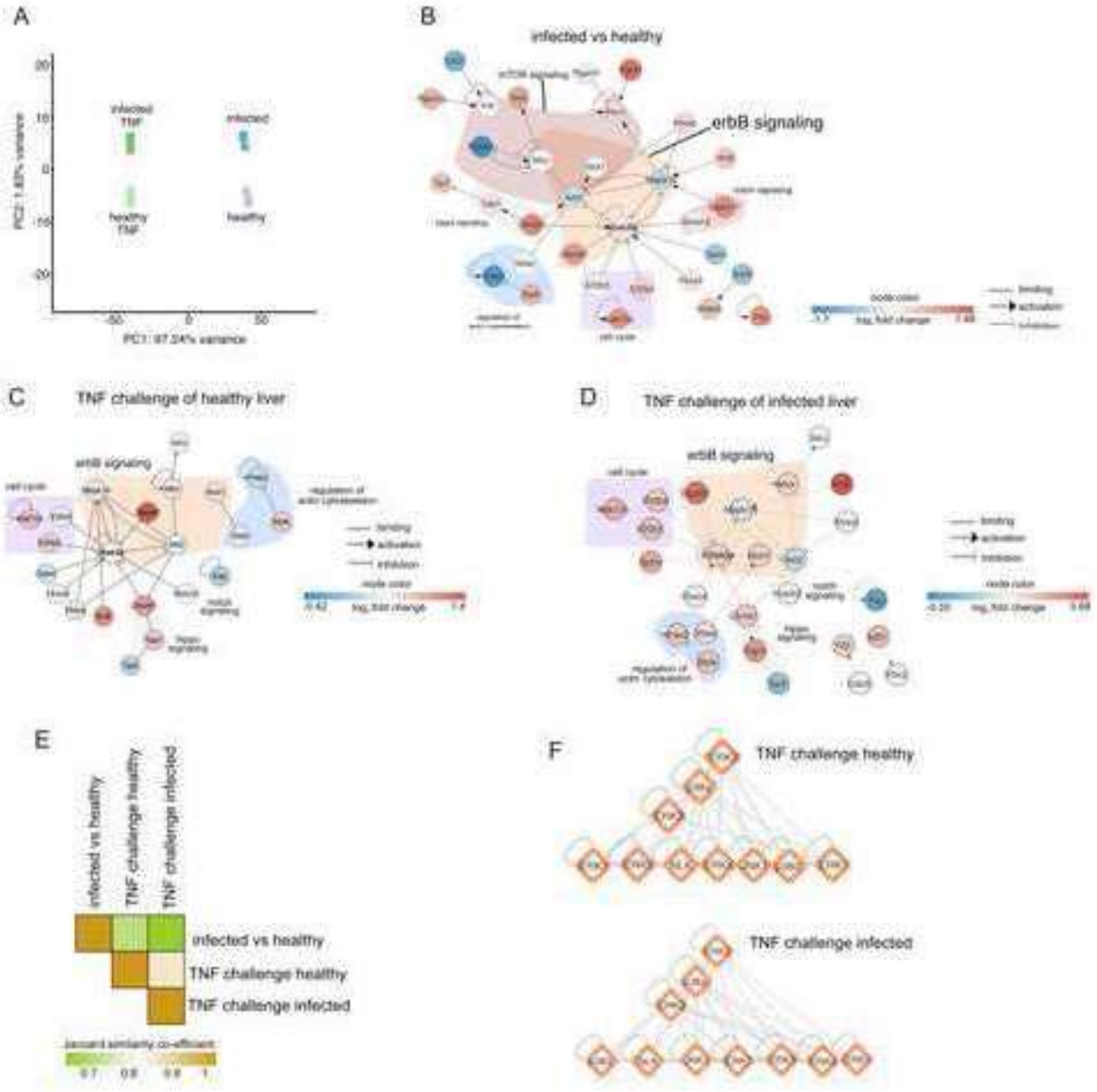

Figure 6

Click here to access/download;Figure;Figure 6 .tiff

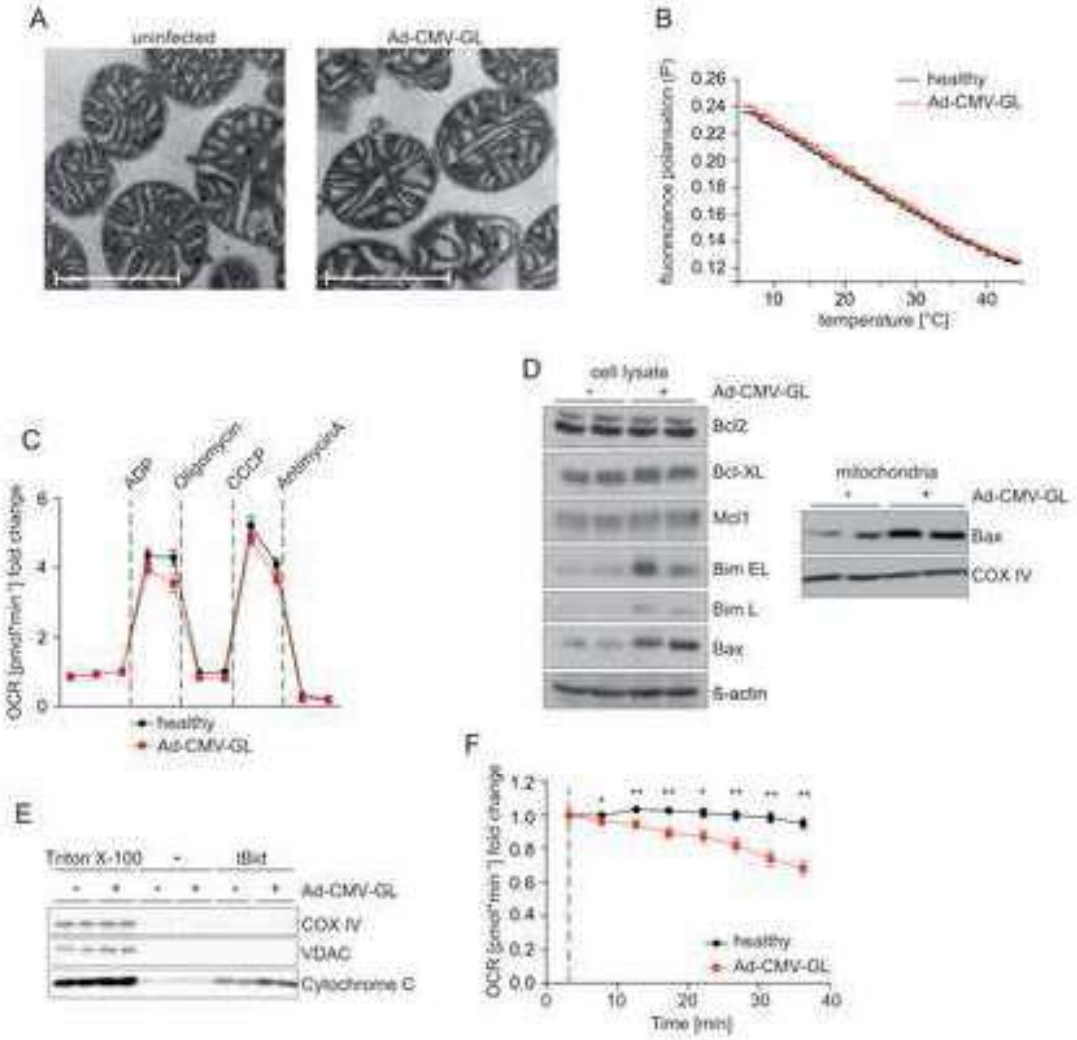

Figure 7

Click here to access/download;Figure;Figure 7 .tiff

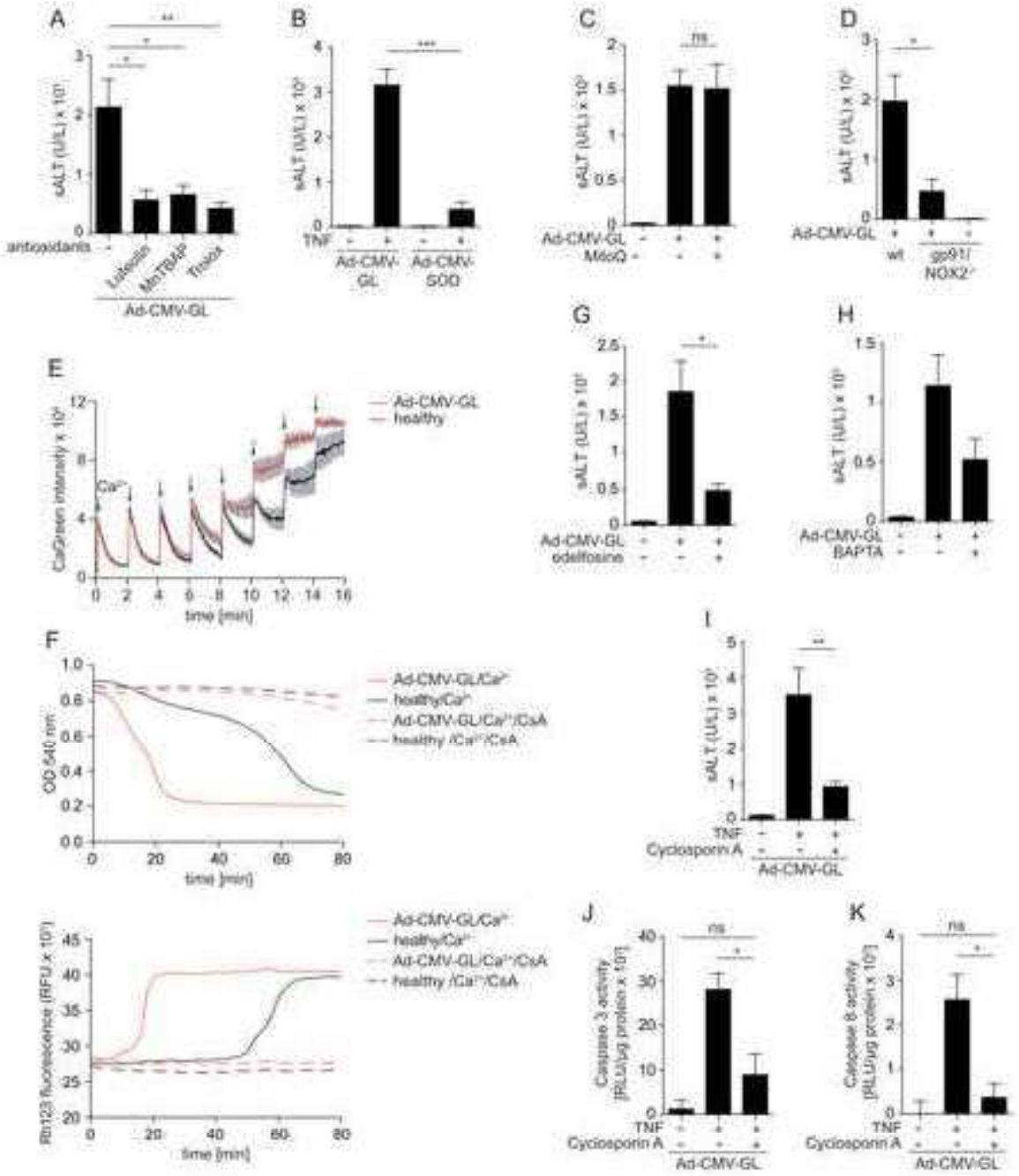

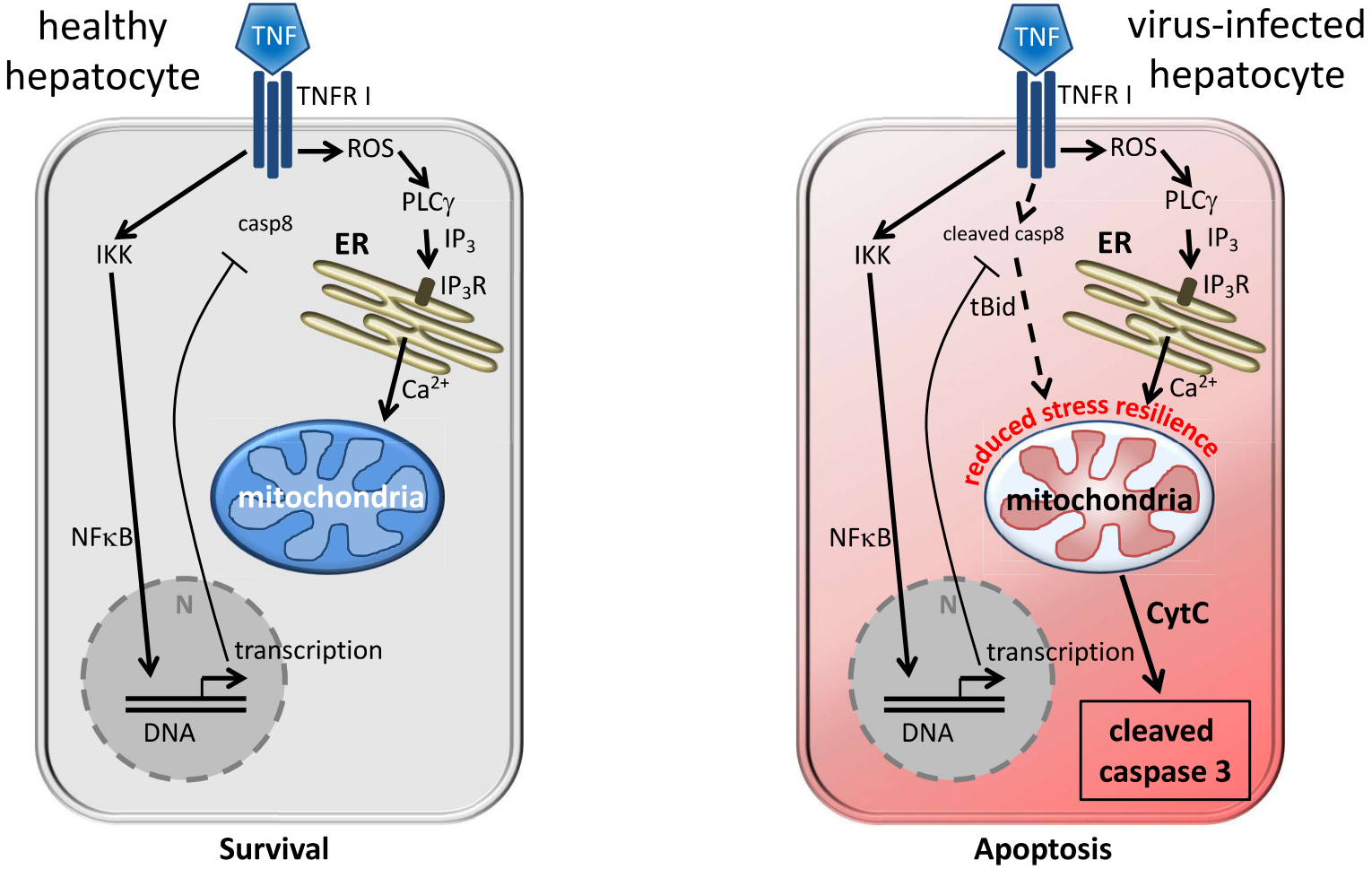
healthy hepatocyte
TNF
TNFR I
ROS
PLCγ
casp8
IKK
ER
IP3
IP3R
Ca2+
mitochondria
NFκB
N
transcription
DNA
Survival
virus-infected hepatocyte
TNF
TNFR I
ROS
PLCγ
cleaved casp8
IKK
ER
IP3
IP3R
tBid
Ca2+
reduced stress resilience
mitochondria
NFκB
N
CytC
transcription
DNA
cleaved caspase 3
Apoptosis